Chapter 3

Port Hamiltonian Control

In this Chapter the port Hamiltonian passivity-based control theory, which will applied to the control of the DFIM and the B2B, is presented. We start with a review of the basic ideas of passivity and of control by interconnection, move to the Interconnection and *Damping Assignment—Passivity-based Control* (IDA-PBC), and finally discuss two improvements of the basic IDA-PBC framework, namely *Simultaneous Interconnection and Damping Assignment* (SIDA), and a variant of the method which improves the robustness of the controller in front of uncertain parameters.

Part of the results of this Chapter can also be found in [7][5][10].

3.1 Introduction

According to one of the accepcions in Webster's [1] "to control" means "to exercise restraint or direction over". In an engineering context, we can translate this to "to stabilize a system in a desired equilibrium point or trajectory". Although a variety of techniques are available for linear control theory (see [26][28][46][47][49] and references therein), most nonlinear control theory revolves around Lyapunov's method and its variants. Lyapunov theory was introduced originally as an analysis tool and became an useful technique for feedback control design.

Lyapunov-based control design is a quite difficult task which involves the construction of a suitable Lyapunov function. This function can be interpreted, in physical systems, as the energy (or storage) function. The main difference between many nonlinear control techniques is the way in which the appropriate Lyapunov function is constructed, as is the case, for instance, of backstepping, forwarding or adaptive control (see [49]). Some other techniques also use the Lyapunov method to design controllers, for instance Sliding Mode Control [80][86], a technique for robust control where the trajectories are forced to reach a sliding surface.

Passivity-based Control (PBC) [63] uses the fact that passive nonlinear systems are described by an storage function (which is a proper Lyapunov function). The control design main goal is then to reshape the original energy function by means of the controller. Based on PBC, the IDA-PBC (Interconnection and Damping Assignment–Passivity-based Control) technique, which uses the passive properties of Port Hamiltonian Systems, was presented in [66] (see also the PhD. Thesis of Hugo Rodríguez [74]).

3.2 Passivity-based control

Traditionally, control problems have been approached adopting a signal-processing viewpoint. This is very useful for linear time-invariant systems, where signals can be discriminated via filtering. However, for nonlinear systems, frequency mixing invalidates this approach due to the following reasons:

- Computations are far from obvious.
- Very complex controls are needed to quench the large set of undesirable signals, and the result is very inefficient, with a lot of energy being consumed and always on the verge of instability (a typical example is provided by bipedal walking machines; see [30]).

Most of the problem stems from the fact that no information about the structure of the system is used. A change of control paradigm is needed, and this can be summarized in the catch expression "control systems as energy exchanging entities". A detailed presentation of this energy-based approach to control is contained in [65] and [66], where complete proofs, which will be mostly omitted here, can be found.

3.2.1 Energy-based control

Definition 3.1. *The map $u \mapsto y$ is passive if there exists a state function $H(x)$, bounded from below, and a nonnegative function $d(t) \geq 0$ such that*

$$\underbrace{\int_0^t u^T(s)y(s)ds}_{\text{energy supplied to the system}} = \underbrace{H(x(t)) - H(x(0))}_{\text{stored energy}} + \underbrace{d(t)}_{\text{dissipated energy}} . \tag{3.1}$$

Example 3.2: a mechanical system

The simplest example of passive system is probably the forced mass-spring-damper arrangement of Figure 3.1, where q is the mass position, $F(t)$ is an external applied force, m is the mass and b and k are the damping and spring coefficients, respectively. One has

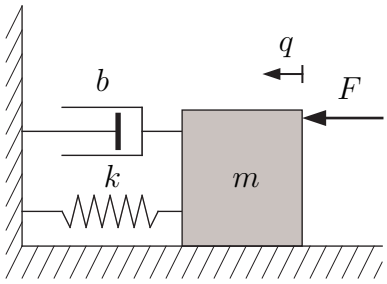

Figure 3.1: Example of a mechanical passive system.

(with $v = \dot{q}$ as mechanical velocity)

$$\begin{aligned}\int_0^t F(s)v(s)\mathsf{d}s &= \int_0^t \left(m\dot{v}(s) + kq(s) + bv(s)\right)\mathsf{d}s \\ &= \left(\frac{1}{2}mv^2(s) + \frac{1}{2}kq^2(s)\right)\Big|_0^t + b\int_0^t v^2(s)\mathsf{d}s \\ &= H(x(t)) - H(x(0)) + b\int_0^t v^2(s)\mathsf{d}s.\end{aligned}$$

Remark 3.3. Notice that, a passive system (3.1), if x^* is a global minimum of $H(x)$ and $d(t) > 0$, and setting $u = 0$, $H(x)$ will decrease in time and the system will reach x^* asymptotically. The rate of convergence can be increased if the energy is extracted from the system with

$$u = -K_{di}y$$

with $K_{di}^T = K_{di} > 0$. △

The key idea of passivity-based control (PBC) is as follows; use feedback

$$u(t) = \beta(x(t)) \tag{3.2}$$

where $\beta(x(t))$ is a function depending on the states, so that the closed-loop system is again a passive system, with new energy function H_d, with respect to $\alpha \mapsto y$, such that H_d has the global minimum at the desired point. Passivity for the closed-loop system is far from obvious: physically, the controller is injecting energy into the system. PBC is robust with respect to unmodeled dissipation, and has built-in safety: even if H is not known exactly, if passivity is preserved, the system will stop somewhere instead of running away and finally blowing up.

With (3.2), H_a is defined as (minus) the energy supplied to the system,

$$H_a = -\int_0^t \beta^T(x(s))y(s),$$

then the closed-loop system has energy function $H_d(x) = H(x) - H_a(x)$. One has the following *energy balance equation* (EBE), which yields an interpretation to PBC:

$$\underbrace{H_d(x(t))}_{\text{closed-loop energy}} = \underbrace{H(x(t))}_{\text{stored energy}} \underbrace{- \int_0^t \beta^T(x(s))y(s).}_{\text{supplied energy}}$$

Remark 3.4. For an affine dynamical system

$$\left\{\begin{array}{rcl}\dot{x} &=& f(x) + g(x)u \\ y &=& h(x)\end{array}\right. ,$$

the EBE is equivalent to the PDE

$$-\beta^T(x)h(x) = \partial H_a\left(f(x) + g(x)\beta(x)\right). \tag{3.3}$$

△

Example 3.5: electrical system

As an example, consider the electrical system in Figure 3.2,

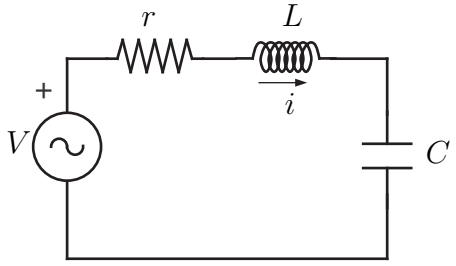

Figure 3.2: Example of an electrical passive system.

$$\dot{x} = \begin{bmatrix} \frac{x_2}{L} \\ -\frac{x_1}{C} - \frac{x_2}{L} r \end{bmatrix} + \begin{bmatrix} 0 \\ 1 \end{bmatrix} V$$

where $x = [q, \lambda]^T$ is the state, $u = V$ is the control input and $y = \frac{\lambda}{L}$ (inductor current) is the passive output. The map $V \mapsto i$ is passive with energy function

$$H(x) = \frac{1}{2C} x_1^2 + \frac{1}{2L} x_2^2$$

and dissipation

$$d(t) = \int_0^t \frac{r}{L^2} x_2^2(s) \mathrm{d}s.$$

Notice that the natural minimum is $[0, 0]$, but forced equilibrium points are of the form $[x_1^*, 0]$. The PDE (3.3) is in this case

$$\frac{x_2}{L} \partial H_a - \left(\frac{1}{C} x_1 + \frac{r}{L} x_2 - \beta(x) \right) \partial H_a = -\frac{1}{L} x_2 \beta(x).$$

Since $x_2^* = 0$ is already a minimum of H, its only necessary to shape the energy in x_1. Hence, taking $H_a = H_a(x_1)$ and solving the above PDE

$$\beta(x_1) = -\frac{\partial H_a}{\partial x_1}$$

i.e. it defines a closed-loop control. Then, one has to choose H_a so that H_d has the minimum at x_1^*. The simplest solution is

$$H_a(x_1) = \frac{1}{2C_a} x_1^2 - \left(\frac{1}{C} + \frac{1}{C_a} \right) x_1^* x_1$$

where C_a is a design parameter. The closed-loop energy H_d can then be computed and it is seen that it has a minimum at $[x_1^*, 0]$ if $C_a > -C$. Finally, the control is computed as

$$u = -\frac{\partial H_a}{\partial x_1} = -\frac{1}{C_a}x_1 + \left(\frac{1}{C} + \frac{1}{C_a}\right)x_1^*.$$

This control is an energy-balancing PBC that stabilizes x^* under stated parameter restrictions.

Example 3.6: electrical system

Consider now the slightly different circuit of Figure 3.3.

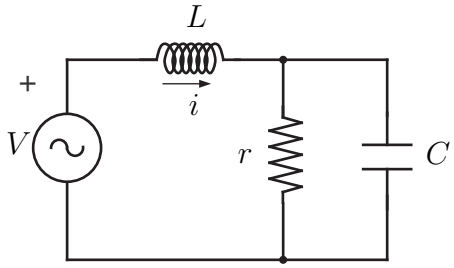

Figure 3.3: Example of an electrical passive system.

With the same states, energy, input and outputs than the preceding system, the equations of the motion are now

$$\dot{x} = \begin{bmatrix} -\frac{1}{rC}x_1 + \frac{1}{L}x_2 \\ -\frac{1}{C}x_1 \end{bmatrix} + \begin{bmatrix} 0 \\ 1 \end{bmatrix} V.$$

Only the dissipation structure has changed, but the admissible equilibria are of the form

$$x^* = [CV^d, \frac{L}{r}V^d]^T$$

for any constant V^d. The power delivered by the source, $p = Vi = V\frac{x_2}{L}$, is nonzero at any equilibrium point except for the trivial one. Hence, the source has to provide an infinite amount of energy to keep any nontrivial equilibrium point, a task which is clearly not feasible. This situation will reappear later into the discussion of invariant and Casimir functions. Notice that pure mechanical systems are free of this problem, since any equilibrium has velocities equal to zero and hence no power in necessary to keep the system at the equilibrium point.

3.2.2 Control as interconnection

To give a physical interpretation of PBC, one can think the controller as a *system exchanging energy with the plant*. Consider two systems, Σ and Σ_c, exchanging energy through an interconnection network given by Σ_l, as depicted in Figure 3.4.

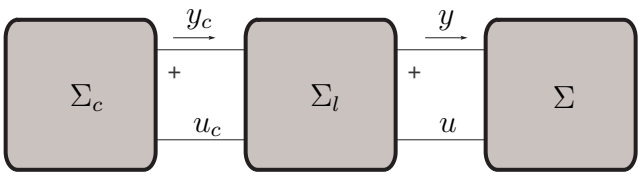

Figure 3.4: Network interpretation of control.

The condition for the interconnection to be power continuous is

$$u_c^T(t)y_c(t) + u^T(t)y(t) = 0 \quad \forall t.$$

Example 3.7: feedback interconnection

As an example, consider the typical negative feedback interconnection displayed in Figure 3.5

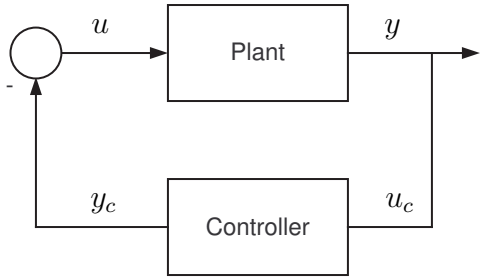

Figure 3.5: Typical negative feedback interconnection.

The interconnection is given by

$$\begin{aligned} u_c &= y \\ u &= -y_c \end{aligned}$$

and is clearly power continuous.

Suppose now that some extra inputs $u \mapsto u + v$, $u_c \mapsto u_c + v_c$ are added to the interconnected system. Then is easy to show the following.

Remark 3.8. Let Σ and Σ_c have the state variables x and ξ. If Σ and Σ_c are passive with energy functions $H(x)$ and $H_c(\xi)$ and Σ_l is power preserving, then the map $[v, v_c] \mapsto [y, y_c]$ is passive for the interconnected system with energy function $H_d(x, \xi) = H(x) + H_c(\xi)$. Or, in short, △

Proposition 3.9. *Power continuous interconnection of passive system yields passive system.*

The resulting system of the interconnection of the plant and the controller is a passive system with energy function

$$H_d(x,\xi) = H(x) + H_c(\xi)$$

but this is not very useful unless the energy function depends only on x. To solve this, the dynamics are restricted to a submanifold of the (x,ξ) space parametrized by x:

$$\Omega_K = (x,\xi); \xi = F(x) + K,$$

and dynamically invariant:

$$(\partial F \dot{x})_{\xi=F(x)+K} = 0.$$

Instead of solving this in general, it is convenient to formulate the problem for a port-controlled Hamiltonian systems.

3.2.3 Casimir functions and the dissipation obstacle

A port-controlled system in explicit form given by (2.1), remind,

$$\left\{ \begin{array}{rcl} \dot{x} & = & (J(x) - R(x))\partial H(x) + g(x)u \\ y & = & g^T(x)\partial H(x) \end{array} \right.$$

with $J^T = -J$, $R^T = R \geq 0$ and $H > 0$, satisfy the following relation

$$\dot{H} = -(\partial H)^T R \partial H + y^T u.$$

Integrating, from 0 to t, the energy balance equation, is recovered

$$H(x(t)) - H(x(0)) = \int_0^t u^T(s) y(s) \mathrm{d}s - \int_0^t (\partial H)^T R \partial H.$$

More precise results about the possibility of obtaining invariant manifolds expressing the controller variables in terms of the variables of the system can be formulated if both systems and controller are PCHS. Let thus

$$\Sigma : \left\{ \begin{array}{rcl} \dot{x} & = & (J(x) - R(x))\partial H(x) + g(x)u \\ y & = & g^T(x)\partial H(x) \end{array} \right.$$

define the plant and

$$\Sigma_c : \left\{ \begin{array}{rcl} \dot{\xi} & = & (J_c(\xi) - R_c(\xi))\partial H_c(\xi) + g_c(\xi)u_c \\ y_c & = & g_c^T(\xi)\partial H_c(\xi) \end{array} \right.$$

define the controller. With the power preserving, standard negative feedback interconnection $u = -y_c$, $u_c = y$, one gets

$$\left[\begin{array}{c} \dot{x} \\ \dot{\xi} \end{array} \right] = \left[\begin{array}{cc} J(x) - R(x) & -g(x)g_c(\xi)^T \\ g_c(\xi)g(x)^T & J_c(\xi) - R_c(\xi) \end{array} \right] \left[\begin{array}{c} \partial H_d(x) \\ \partial H_d(\xi) \end{array} \right]$$

where $H_d(x,\xi) = H(x) + H_c(\xi)$. Let us look now for invariant manifolds of the form

$$C_K(x,\xi) = F(x) - \xi + K.$$

Condition $\dot{C}_K = 0$ yields

$$[\partial F, I_m]^T \begin{bmatrix} J(x) - R(x) & -g(x)g_c(\xi)^T \\ g_c(\xi)g(x)^T & J_c(\xi) - R_c(\xi) \end{bmatrix} \begin{bmatrix} \partial H_d(x) \\ \partial H_d(\xi) \end{bmatrix} = 0.$$

In order to keep the freedom to choose H_c, one demands that the above equation is satisfied on C_K for every Hamiltonian, *i.e.* one imposes on F the following system of PDE's:

$$[\partial F, I_m]^T \begin{bmatrix} J(x) - R(x) & -g(x)g_c(\xi)^T \\ g_c(\xi)g(x)^T & J_c(\xi) - R_c(\xi) \end{bmatrix} = 0.$$

Functions $C_K(x,\xi)$ such that F satisfies the above PDE on $C_K = 0$ are called Casimir. They are invariants associated to the structure of the system (J, R, g, J_c, R_c, g_c), independently of the Hamiltonian function.

One can show [66] that the PDE for F has solution iff, on $C_K = 0$,

1. $(\partial F)^T J \partial F = J_c$,
2. $R\partial F = 0$,
3. $R_c = 0$,
4. $(\partial F)^T J = g_c g^T$.

Conditions 2 and 3 are easy to understand: essentially, no Casimir functions exist in presence of dissipation. Given the structure of the PDE, $R_c = 0$ is unavoidable, but one can have an effective $R = 0$ just by demanding that the coordinates on which the Casimir depends do not have dissipation, and hence condition 2.

If the preceding conditions are fulfilled, an easy computation shows that the dynamics on C_K is given by

$$\dot{x} = (J(x) - R(x))\partial H_d$$

with $H_d(x) = H(x) + H_c(F(x) + K)$. Notice that, due to condition 2,

$$R\partial H_c(F(x) + K) = \underbrace{R(\partial F)}_{=0} \frac{\partial H_c}{\partial \xi}(F(x) + K) = 0,$$

so, in energy-balancing PBC, dissipation is only admissible for those coordinates which do not require energy shaping.

For regulation problems in mechanical systems, where the state consists of positions and velocities, dissipation only appear associated to the later, while energy shaping is necessary only in the position part, since the kinetic energy already has the minimum at the desired point (that is, at velocity equal to zero). Hence, the dissipation obstacle is always absent for mechanical regulation problems. For the first of the two simple RLC circuits considered previously (Figures 3.2 and 3.3), dissipation appears in a coordinate, x_2, which already has the minimum at the desired point. For the second one, the minimum of the energy has to be moved for both coordinates, and hence the dissipation obstacle is unavoidable.

3.3 Interconnection and damping assignment – Passivity-based control

The Interconnection and damping assignment–Passivity-based control (IDA-PBC) was introduced in [66] to combine the passivity properties of PCHS with control by interconnection and energy-based control. This technique has been applied to many different plants: mechanical systems [2][64], magnetic levitation systems [77][78], mass-balance systems [60], electric machines [12][73], power converters [39][76]. An extended survey of the IDA-PBC methodology with examples is presented in [62].

The key idea is that using the Hamiltonian framework, solving the PDE associated to the energy-balance equation (3.3) can be done with an appropriate selection of the interconnection J and dissipation R matrices and the energy function H of the desired closed-loop system (which will be denoted with subindex d: J_d, R_d and H_d).

3.3.1 IDA-PBC technique

The previous Section has exposed some shortcomings of the passivity based control by means of control-as-interconnection. One can get a method with more freedom if not only the energy function is changed but also the interconnection J and dissipation R, *i.e.* if one aims at a closed-loop system of the form

$$\dot{x} = (J_d(x) - R_d(x))\partial H_d(x), \tag{3.4}$$

where $J_d = -J_d^T$ is the *desired* interconnection matrix, $R_d = R_d^T \geq 0$ is the *desired* dissipation matrix and H_d (with a minimum at x^*) is the *desired* Hamiltonian function.

Proposition 3.10. *Consider the system* [a]

$$\dot{x} = f(x) + g(x)u. \tag{3.5}$$

Assume there are matrices $J_d = -J_d^T$, $R_d = R_d^T \geq 0$ and a smooth function H_d that verify the so-called matching equation

$$f(x) + g(x)u = (J_d(x) - R_d(x))\partial H_d(x). \tag{3.6}$$

Then the closed-loop system with control $u = \beta(x)$,

$$\beta(x) = (g^T(x)g(x))^{-1}g^T(x)\left((J_d(x) - R_d(x))\partial H_d(x) - f(x)\right) \tag{3.7}$$

is asymptotically stable.

[a] Historically [66] the plant was described as a PCHS, but in a more general case the method is also valid for an affine dynamical system with the form (3.5).

Proof. Substituting (3.7) into (3.5) the closed-loop system becomes

$$\dot{x} = (J_d(x) - R_d(x))\partial H_d,$$

which, following Proposition 1, is asymptotically stable. □

It is thus clear that the problem is how to solve the matching equation (3.6). Notice that there is a huge amount of freedom in selecting J_d, R_d and H_d satisfying the previous

assumptions ($J_d = -J_d^T$, $R_d = R_d^T \geq 0$ and $x^* = \arg\min H_d$). Several techniques have been proposed in the literature (discussed in detail in [62]):

- In **Non-Parameterized IDA** (see [39][65][76]), the structure and damping matrices ($J_d(x)$ and $R_d(x)$) are fixed, the matching equation is pre-multiplied by a left annihilator of $g(x)$ and the resulting PDE in H_d is then solved.
- In **Algebraic IDA**, (see [37]), the desired Hamiltonian function H_d is first selected (for example a quadratic function in the error terms) and then the resulting algebraic equations are solved for J_d and R_d.
- In **Parameterized IDA**, applicable mainly to underactuated mechanical systems, (see [64]), the knowledge of a priori structure of the desired Hamiltonian is used to obtain a more easy to solve PDE, giving constraints on J_d and R_d.
- In **Interlaced Algebraic-Parameterized IDA**, (see [61]), the PDE is evaluated in some subspace (where the solution can be easily computed) and then matrices J_d, R_d are found which ensure a valid solution of the matching equation.

There is not a *best* method to solve the matching equation. Each control problem requires an individual study to find out which of the above strategies provides an acceptable solution of the matching equation.

The first papers on IDA-PBC (see for example [66]) introduced new matrices J_a, R_a and a Hamiltonian function H_a such that

$$\begin{aligned} J_d(x) &\triangleq J(x) + J_a(x), \\ R_d(x) &\triangleq R(x) + R_a(x), \\ H_d(x) &\triangleq H(x) + H_a(x) \end{aligned}$$

referred to as the structure matrix, damping matrix and Hamiltonian function, respectively, contributed by the controller. With this notation, and using a PCHS description of the system (3.5), the matching equation (3.6) becomes

$$(J(x) + J_a(x) - R(x) - R_a(x))\partial H_a = -(J_a(x) - R_a(x))\partial H + g(x)u, \tag{3.8}$$

where the available degrees of freedom for the design are the matrices are J_a, R_a and the function H_a.

In order to clarify the methodology, and to compare later the classic IDA-PBC controllers to the designed ones using the new approaches presented in this Thesis (see subsection 3.3.2 and Section 3.4), we present here two examples: a classical DC motor and a nonlinear toy model.

Example 3.11: a DC motor

Consider a permanent magnet DC motor (or either a field DC motor for which the field dynamics, λ_f, is neglected). From the PCHS model of the DC motor presented in Section 2.2, and using $K = L_{Af} i_f = ct$, called the torque constant, the port-controlled Hamiltonian system is described by

$$\dot{x} = (J - R)\partial H(x) + g + g_u u$$

with the variables $x \in \mathbb{R}^2$

$$x = [\lambda, p_m]^T$$

where λ is the inductor flux (or λ_a in the generic case), and p_m is the angular momentum. The interconnection, dissipation and port matrices are

$$J = \begin{bmatrix} 0 & -K \\ K & 0 \end{bmatrix} \quad R = \begin{bmatrix} r & 0 \\ 0 & B_r \end{bmatrix} \quad g = \begin{bmatrix} 0 \\ -\tau_L \end{bmatrix} \quad g_u = \begin{bmatrix} 1 \\ 0 \end{bmatrix}$$

with the control input $u = v$ (to simplify the notation the voltage v_a of section 2.2, in now called v). Notice that the system inputs have been split according to whether they can be controlled or not when the machine acts as a motor. In this case, the mechanical torque can be seen as an external perturbation. r and B_r represent the electrical and mechanical losses respectively, and the Hamiltonian function is given by

$$H(x) = \frac{1}{2L}\lambda^2 + \frac{1}{2J_m}p_m^2,$$

where L is the inductance and J_m the inertia of the motor.

Assume that the control objective is a desired speed ω^d. In terms of ω^d, the equilibrium values of i and v are

$$\begin{aligned} i^* &= \frac{1}{K}(B_r\omega^d + \tau_L) \\ u^* &= ri^* + K\omega^d. \end{aligned}$$

To apply the IDA-PBC technique (following the algebraic approach) a desired Hamiltonian function H_d is fixed as

$$H_d(x) = H(x) = \frac{1}{2L}(\lambda - \lambda^*)^2 + \frac{1}{2J_m}(p_m - p_m^*)^2,$$

which implies (recall the energy and co-energy variables relationship, $\lambda = Li$ and $p_m = J_m\omega$)

$$\partial H_d = \begin{bmatrix} i - i^* \\ \omega - \omega^d \end{bmatrix}.$$

In order to solve the matching equation of the IDA-PBC method, we consider generalized interconnection and dissipation matrices given by

$$J_d - R_d = \begin{bmatrix} -r_d & -j_d \\ j_d & -b_d \end{bmatrix}. \tag{3.9}$$

The first row of the matching equation will yield the desired control action, while the second row imposes

$$j_d(i - i^*) - b_d(\omega - \omega^d) = Ki - B_r\omega - \tau_L.$$

Setting $b_d = B_r$, and using the equilibrium point expression, j_d is computed as

$$j_d = K,$$

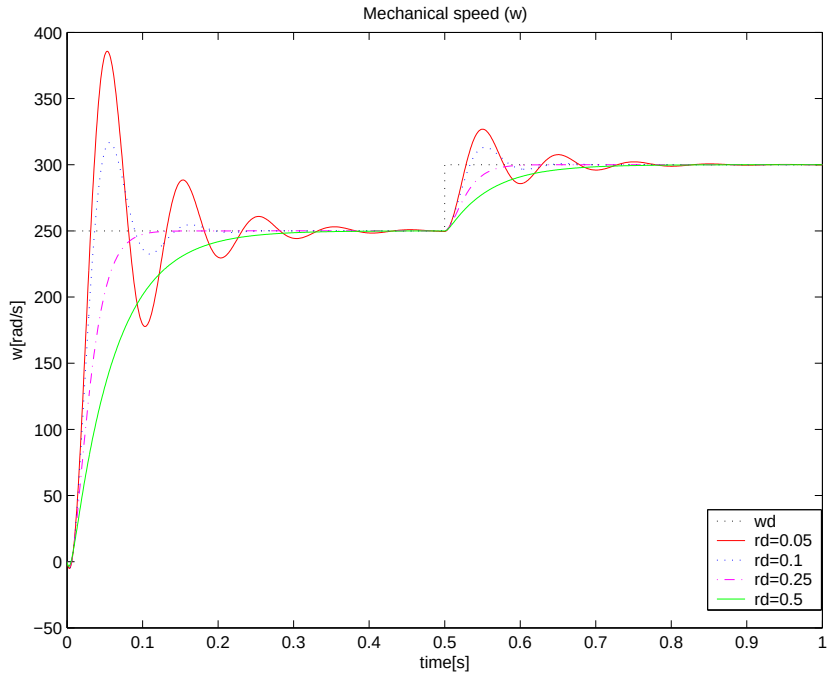

Figure 3.6: Simulation results: Mechanical speed ω, for different r_d values.

where r_d is a still free parameter to tune the controller. Finally, substituting into the first row of the matching equation,

$$u = -r_d(i - i^*) - ri + K\omega^d. \tag{3.10}$$

Notice that this is just a proportional + constant compensation controller.

Figures 3.6-3.8 show the system behaviour with the control law (3.10). The motor parameters are: $r = 0.05\Omega$, $L = 2$mH, $K = 0.07$N·m·A^{-1}, $B_r = 0.0001$N·m·rad^{-1}s^{-1}, $J_m = 0.0006$Kg·m^2 and the nominal torque is $\tau_L = 2$N·m. The desired mechanical speed is fixed at $\omega_d = 250$rad·s^{-1} for $0\text{s} < t \leq 0.5\text{s}$ and changes at $\omega_d = 300$rad·s^{-1} for $0.5\text{s} < t \leq 1\text{s}$.

Figure 3.6 shows the mechanical speed for different damping r_d values. Notice that for a higher value of r_d the transient becomes more damped, which gives a physical interpretation of the R_d matrix (3.9). Figure 3.7 shows the inductor current i, with a similar behaviour to that of ω. Finally, the space-state trajectory for $0\text{s} < t \leq 0.5\text{s}$, which converges to the equilibrium point, is depicted in Figure 3.8

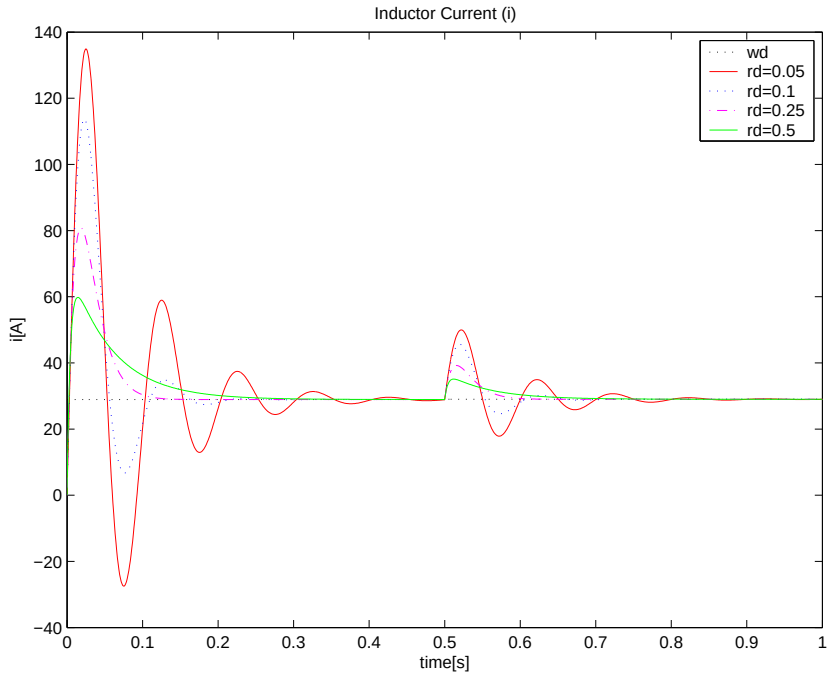

Figure 3.7: Simulation results: Inductor current i, for different r_d values.

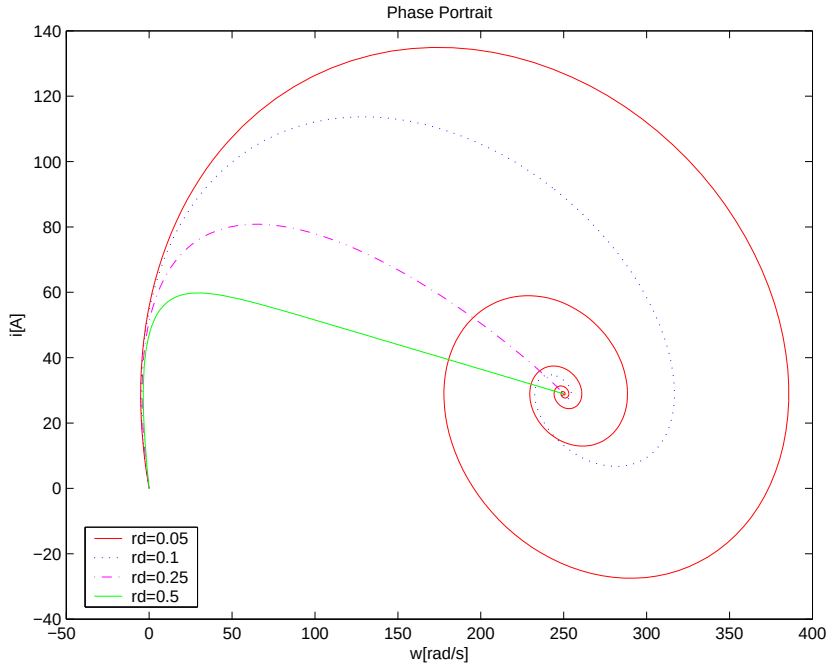

Figure 3.8: Simulation results: State space $[\omega, i]$ trajectory, for different r_d values.

Example 3.12: a toy model

Consider the following 2-dimensional nonlinear control system (presented in [10])

$$\begin{aligned} \dot{x}_1 &= -x_1 + \xi x_2^2, \\ \dot{x}_2 &= -x_1 x_2 + u, \end{aligned} \tag{3.11}$$

where $\xi > 0$. This can be cast into PCHS form

$$\dot{x} = (J - R)\partial H + gu \tag{3.12}$$

with

$$J = \begin{bmatrix} 0 & x_2 \\ -x_2 & 0 \end{bmatrix}, \quad R = \begin{bmatrix} 1 & 0 \\ 0 & 0 \end{bmatrix}, \quad g = \begin{bmatrix} 0 \\ 1 \end{bmatrix}$$

$$H(x) = \frac{1}{2}x_1^2 + \frac{1}{2}\xi x_2^2.$$

The control objective is to regulate, for example, x_2 to a desired value x_2^d (nevertheless the control law for a regulated x_1 yields the same control law). The equilibrium of (3.11) corresponding to this is given by

$$x_1^* = \xi(x_2^d)^2, \quad u^* = \xi(x_2^d)^3.$$

Using the IDA-PBC technique, also within the algebraic approach, we match (3.12) to

$$\dot{x} = (J_d - R_d)\partial H_d$$

with

$$J_d = \begin{bmatrix} 0 & \alpha(x) \\ -\alpha(x) & 0 \end{bmatrix}, \quad R_d = \begin{bmatrix} 1 & 0 \\ 0 & r \end{bmatrix},$$

and

$$H_d(x) = \frac{1}{2}(x_1 - x_1^*)^2 + \frac{1}{2\gamma}(x_2 - x_2^d)^2,$$

where $\alpha(x_1, x_2)$ is a function to be determined by the matching procedure and $\gamma > 0$, $r > 0$ are adjustable parameters.

From the first row of the matching equation $(J - R)\partial H + gu = (J_d - R_d)\partial H_d$ one gets

$$-x_1 + \xi x_2^2 = -(x_1 - x_1^*) + \frac{\alpha}{\gamma}(x_2 - x_2^d),$$

from which

$$\alpha(x_1, x_2) = \frac{\gamma}{x_2 - x_2^d}(\xi x_2^2 - x_1^*) = \gamma\xi(x_2 + x_2^d).$$

Substituting this into the second row of the matching equation

$$-x_1 x_2 + u = -\alpha(x_1 - x_1^*) - \frac{r}{\gamma}(x_2 - x_2^d),$$

yields the feedback control law

$$u = x_1 x_2 - \gamma\xi(x_1 - x_1^*)(x_2 + x_2^d) - \frac{r}{\gamma}(x_2 - x_2^d). \tag{3.13}$$

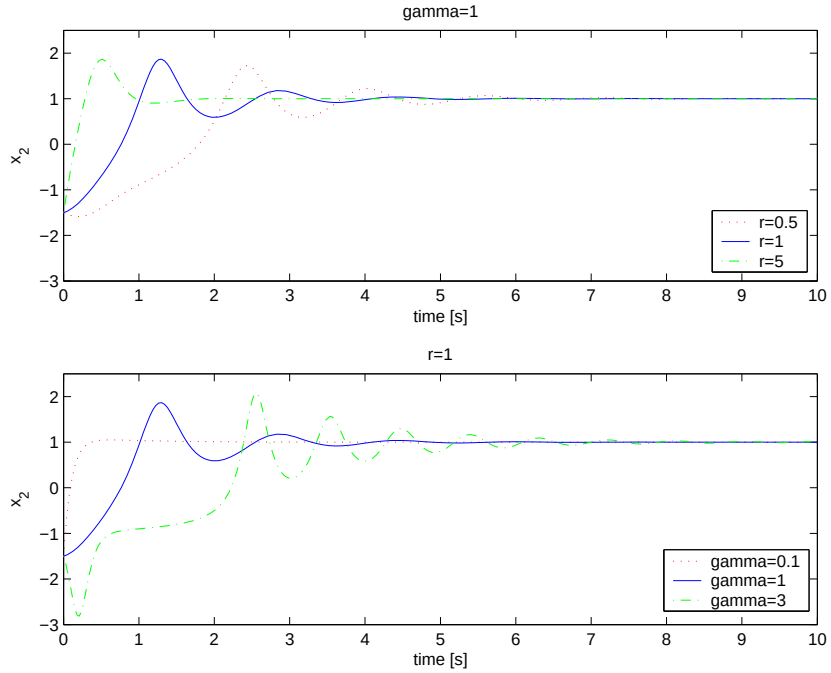

Figure 3.9: Simulation results: x_2 behaviour for different r and γ values.

This control law yields a closed-loop system which is Hamiltonian with (J_d, R_d, H_d), and which has (x_1^*, x_2^d) as a globally asymptotically stable equilibrium point.

Figures 3.9 to 3.12 show the behavior of the system controlled by the IDA-PBC controller (3.13). The parameters are $\xi = 2$ and $x_2^d = 1$. Figures 3.9 and 3.10 show $x_2(t)$ and $x_1(t)$ for different r and γ values, while in Figures 3.11 and 3.12 the phase portrait is depicted. Notice that the γ parameter has more influence on the trajectories. This is due to the fact that γ modifies the Hamiltonian in the x_2 direction (see Figure 3.13) and tuning this parameter makes trajectories of x_2 restricted (or semi-bounded).

3.3.2 Simultaneous IDA-PBC

The standard two–stage procedure used in IDA-PBC, consisting of splitting the control action into the sum of energy-shaping and damping injection terms, is not without loss of generality, and effectively reduces the set of systems that can be stabilized with IDA–PBC. This assertion is, of course, not surprising since it is clear that, to achieve strict passivity, the procedure described above is just one of many other possible ways. This point is illustrated with the IDA–PBC design methodology proposed in [66] (see the previous subsection). To enlarge the set of systems that can be stabilized via IDA–PBC we suggest to carry out *simultaneously* the energy shaping and the damping injection stages and refer to this variation of the method as SIDA–PBC.

As we said before, the key for the success of IDA-PBC is the solution of the matching

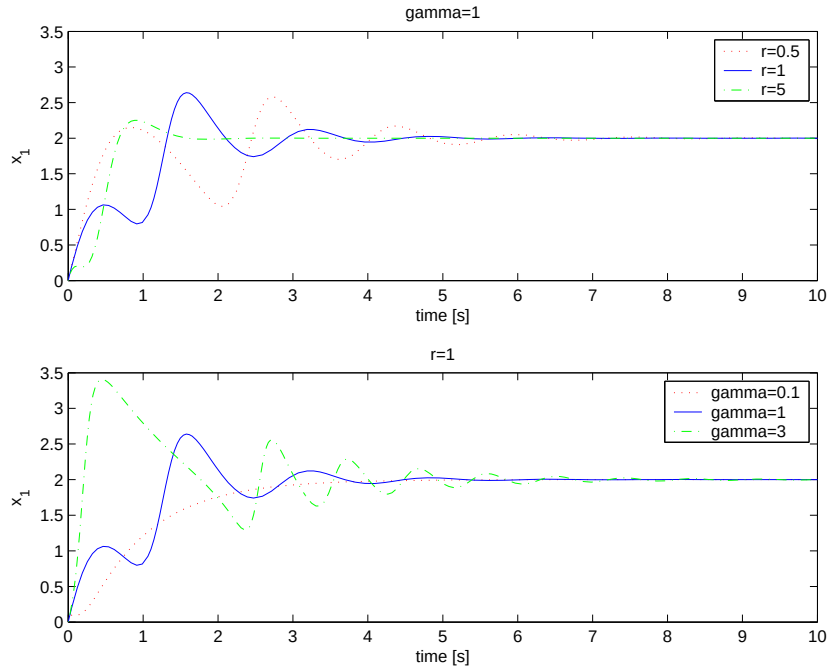

Figure 3.10: Simulation results: x_1 behaviour for different r and γ values.

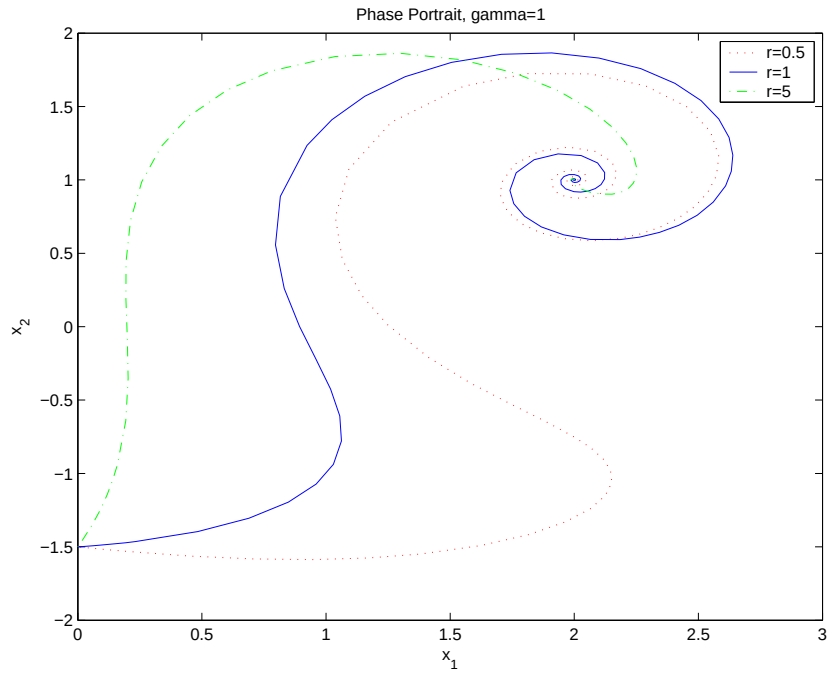

Figure 3.11: Simulation results: State space $[x_1, x_2]$ trajectory, for different r values.

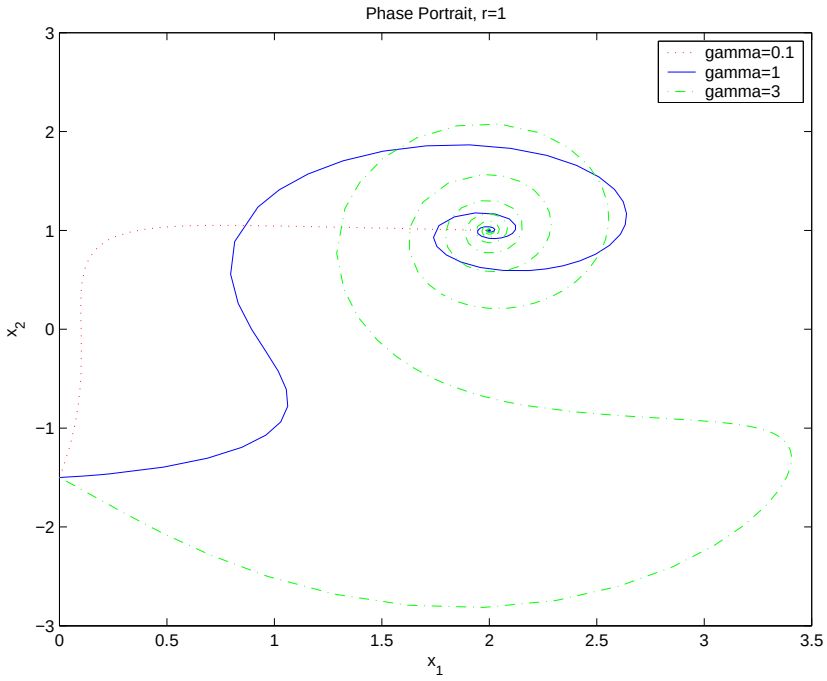

Figure 3.12: Simulation results: State space $[x_1, x_2]$ trajectory, for different γ values.

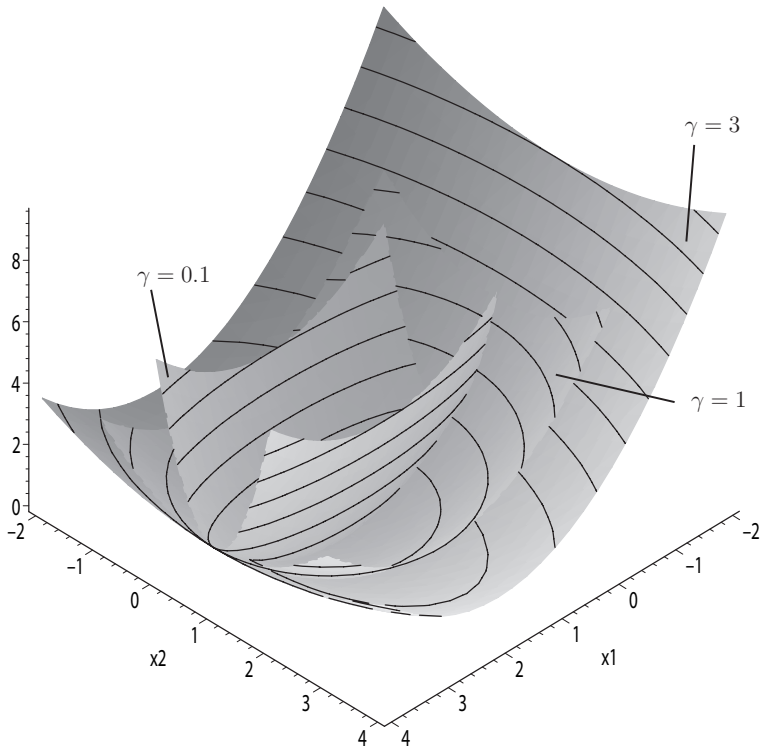

Figure 3.13: Desired Hamiltonian function H_d for different γ values.

equation

$$f(x) + g(x)u = (J_d - R_d)\partial H_d. \tag{3.14}$$

With the motivation of enlarging the class of systems for which this equation is solvable we propose to avoid the decomposition of the control into energy–shaping and damping injection terms. Instead, we suggest to carry out *simultaneously* both stages and replace (3.14), with the SIDA–PBC matching equations

$$f(x) + g(x)u = F_d(x)\partial H_d, \tag{3.15}$$

and to replace the constraints

$$J_d^T(x) = -J_d(x), \quad R_d(x) = R_d(x)^T \geq 0 \tag{3.16}$$

by the *strictly weaker* condition

$$F_d(x) + F_d^T(x) \leq 0, \tag{3.17}$$

and define the control as

$$u = [g^T(x)g(x)]^{-1}g^T(x)(F_d(x)\partial H_d - f(x)). \tag{3.18}$$

Since the set of skew–symmetric matrices is strictly contained in the set of matrices with negative semi–definite symmetric part, it is clear that the set of functions $\{f(x), g(x)\}$ for which (3.14) (subject to the constraint (3.16)) is solvable is strictly smaller than the set for which (3.15), subject to (3.17), is solvable.

Remark 3.13. Similarly to IDA–PBC, application of SIDA–PBC also yields a closed–loop PCH system of the form (3.4) with

$$J_d(x,t) = \frac{1}{2}[F_d(x,t) - F_d^T(x,t)], \quad R_d(x,t) = \frac{1}{2}[F_d(x,t) + F_d^T(x,t)].$$

△

The SIDA-PBC can be summarized in the following Proposition.

Proposition 3.14. *A dynamical system in an affine the form*

$$\dot{x} = f(x) + g(x)u,$$

with the control law (3.18)

$$u = [g^T(x)g(x)]^{-1}g^T(x)(F_d(x)\partial H_d - f(x)),$$

is asymptotically stable to x^* iff

$$x^* = \arg\min H_d$$

and

$$F_d(x) + F_d(x)^T \leq 0.$$

Example 3.15: a toy model

Now we apply this technique to the toy model described before. We have to solve the new matching equation (3.15), which implies the control law (3.18). The model (3.11) can be written in the form $\dot{x} = f(x) + g(x)u$ with

$$f(x) = \begin{bmatrix} -x_1 + \xi x_2^2 \\ -x_1 x_2 \end{bmatrix}, \quad g = \begin{bmatrix} 0 \\ 1 \end{bmatrix}.$$

Splitting the F_d matrix as

$$F_d = \begin{bmatrix} F_{11} & F_{12} \\ F_{21} & F_{22} \end{bmatrix},$$

the control law (3.18) has the following form

$$u = F_{21}\partial_{x_1} H_d + F_{22}\partial_{x_2} H_d + x_1 x_2$$

where F_{21} and F_{22} are free parameters satisfying (3.17) and $x^* = \arg\min H_d(x)$. Notice that we have more degrees of freedom than in the conventional IDA-PBC technique.

In this case the more evident choice is to take a quadratic energy function, for example

$$H_d = \frac{1}{2}(x_1 - x_1^*)^2 + \frac{\xi}{2}(x_2 - x_2^*)^2$$

which implies

$$\partial_{x_1} H_d = x_1 - x_1^*, \text{ and } \partial_{x_2} H_d = \xi(x_2 - x_2^*).$$

Setting $F_{21} = -x_2$ and $F_{22} = -\frac{k}{\xi}$, the control law yields

$$u = x_1^* x_2 - k(x_2 - x_2^*). \tag{3.19}$$

The F_{11} and F_{12} are still free and must satisfy the matching equation for the x_1 dynamics,

$$-x_1 + \xi x_2^2 = F_{11}(x_1 - x_1^*) + F_{12}\xi(x_2 - x_2^*).$$

In order to simplify the calculations, we set $F_{11} = -1$, which implies

$$F_{22} = x_2 + x_2^*.$$

Finally, to prove stability we only have to be sure that the $F + F^T$ matrix is negative-semidefinite, *i.e.*

$$F + F^T = \begin{bmatrix} -2 & x_2^* \\ x_2^* & -\frac{k}{\xi} \end{bmatrix} \leq 0$$

and, applying Schur's inequality,

$$k \geq \frac{1}{4}\xi x_2^{*2} = \frac{1}{4}x_1^*.$$

Figure 3.14 shows the simulation results of the control law (3.19). The parameter values are $\xi = 2$, $x_2^d = 2$ and $k = 1$. Notice that the system goes to the desired fixed point x^*.

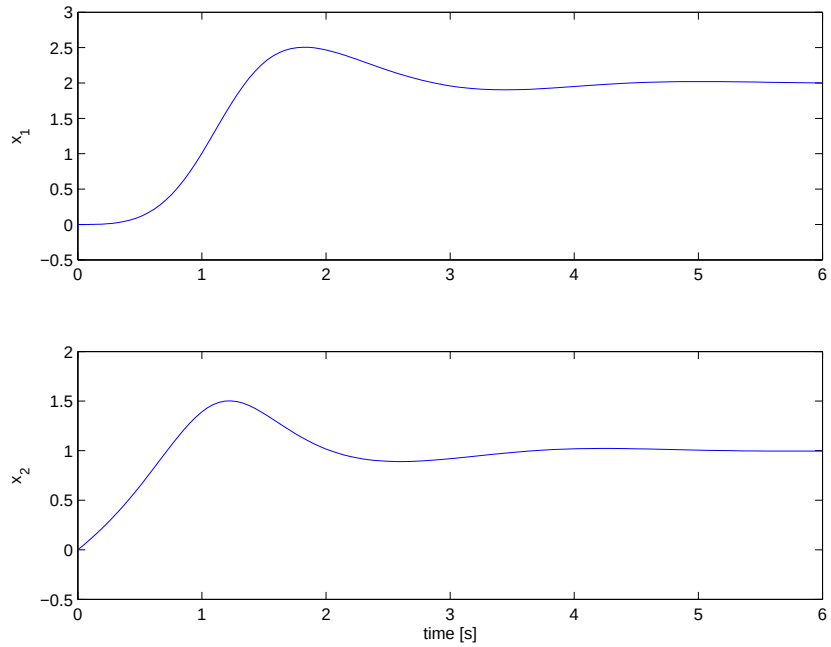

Figure 3.14: Simulation results: x_1 and x_2 for a SIDA-PBC controller.

3.4 Improving the robustness of the IDA-PBC technique

One of the problems of the IDA-PBC technique for practical applications is the robustness of the designed controllers.

The input disturbance suppression for PCHS, using an internal model, is studied in [40]. In [78] an IDA-PBC controller for a magnetic levitation system was experimentally tested. In this case, the robustness problem was partially solved adding an integral term to the error of the passive output. This dynamical extension partially solves the problem for relative degree one outputs but the main problem remains open for higher relative degree outputs [10]. In this case the dynamical extension is not clear because, in general, it breaks the skew-symmetric property of the J_d matrix.

3.4.1 Adding an integral term

In this subsection we explain why the integral term can be used in a PCHS framework for relative degree one outputs, or in other words, passive outputs. To expose the basic idea, consider a fully actuated control system of the form

$$\begin{cases} \dot{x}_1 = f_1(x_1, x_2) \\ \dot{x}_2 = f_2(x_1, x_2) + g(x_1, x_2)u \end{cases} \tag{3.20}$$

where $x_1 \in \mathbb{R}^n$, $x_2 \in \mathbb{R}^m$ and $u \in \mathbb{R}^m$, and g is full rank. Assume the IDA-PBC technique can be applied to (3.20) so that in closed-loop the system becomes[1]

$$\begin{bmatrix} \dot{x}_1 \\ \dot{x}_2 \end{bmatrix} = \begin{bmatrix} J_d - R_d \end{bmatrix} \begin{bmatrix} \partial_1 H_d \\ \partial_2 H_d \end{bmatrix}$$

[1]To simplify the notation ∂_{x_s} is written as ∂_s, where s is the subindex of x.

with control law

$$u = g^{-1}\left((O_{m\times n} \quad I_{m\times m})(J_d - R_d)\partial H_d - f_2\right).$$

Under the stated assumptions, the x_2 are relative degree one outputs. We can easily add a dynamical extension to them by means of

$$\dot{z} = -a\partial_2 H_d, \tag{3.21}$$

where $a \in \mathbb{R}^{m\times m}$, see [36][78]. The whole closed loop system can be rewritten in Hamiltonian form as

$$\begin{bmatrix} \dot{x}_1 \\ \dot{x}_2 \\ \dot{z} \end{bmatrix} = \begin{bmatrix} J_d - R_d & 0 \\ 0 \quad -a & a^T \\ & 0 \end{bmatrix} \begin{bmatrix} \partial_1 H_{dz} \\ \partial_2 H_{dz} \\ \partial_z H_{dz} \end{bmatrix}$$

with a new Hamiltonian function

$$H_{dz} = H_d + \frac{k}{2} z^T z.$$

The new controller is

$$v = u + g^{-1} k a^T z = u - g^{-1} k a^T a \int \partial_2 H_{dz}.$$

Notice that (3.21) forces $x_2 = x_2^*$ to remain a fixed point of the extended system.

The same procedure, when applied to the higher relative degree output x_1, requires a closed loop system of the form

$$\begin{bmatrix} \dot{x}_1 \\ \dot{x}_2 \\ \dot{z} \end{bmatrix} = \begin{bmatrix} J_d - R_d & 0 \\ -a \quad 0 & b \\ & 0 \end{bmatrix} \begin{bmatrix} \partial_1 H_{dz} \\ \partial_2 H_{dz} \\ \partial_z H_{dz} \end{bmatrix}$$

where now $a \in \mathbb{R}^{n\times n}$ and $b \in \mathbb{R}^{m\times n}$. The a term is used to force the equilibrium point x_1^* of the output, while b is necessary to put the integral action into the control law. In this case stability cannot be proved using the PCHS properties, since the a, b terms break the semi-definite positiveness of the dissipation matrix:

$$R_{dz} = \begin{bmatrix} R_d & a^T/2 \\ a/2 \quad -b^T/2 & -b/2 \\ & 0 \end{bmatrix}.$$

Indeed, consider a matrix of the form

$$M = \begin{bmatrix} A & B^T \\ B & D \end{bmatrix}.$$

A simple application of Schur's complement shows that if $D = 0$, then $B \neq 0$ implies $M < 0$. In our case, this would mean $a = 0$ and $b = 0$, which makes no sense.

3.4.2 Influence of unknown parameters on the PCHS structure

In this subsection we point out the kind of problems that can appear in the closed-loop structure obtained by IDA-PBC methods for relative degree one outputs, when nominal values are used in a system with uncertain parameters.

Although the IDA-PBC method has some built-in robustness coming from its PCHS structure, the use of a nominal u for systems with uncertain parameters can give a closed-loop system which is not exactly PCHS. One may thing that for nominal parameters in a small neighborhood of the actual ones, the "$J-R$" structure will not be destroyed; however, we will see that the resulting closed-loop system has interconnection and dissipation matrices depending on the state of the system, even if the closed-loop system for the actual parameter values does not; this has as a consequence that the effect of small parameter changes is not uniform in state space and, in particular, is unbounded in a neighborhood of the desired regulation point. In addition to this, the closed-loop system obtained with a nominal control does not have, in general, x^* as a fixed point. As is well known from elemental control theory, this last problem can be corrected by adding control terms proportional to the integral of the error. Integral control has been discussed in the PCHS setting in the previous subsection 3.4.1, where it is shown that adding as state variable the integral of the natural passive output of the closed-loop system yields a system which is again PCHS.

Consider the dynamical system (3.20) of subsection 3.4.1,

$$\begin{cases} \dot{x}_1 = f_1(x_1, x_2) \\ \dot{x}_2 = f_2(x_1, x_2) + g(x_1, x_2)u \end{cases} \tag{3.22}$$

where $x_1 \in \mathbb{R}^n$, $x_2 \in \mathbb{R}^m$, $u \in \mathbb{R}^m$ and $\det g \neq 0$, so that the x_2 are relative degree one outputs which we want to regulate to desired values x_2^*. Given x_2^*, the fixed point values of x_1 and u are obtained by equaling to zero the right-hand sides of (3.22).

Applying the IDA-PBC technique, we match the system to the desired partitioned PCHS

$$\begin{bmatrix} \dot{x}_1 \\ \dot{x}_2 \end{bmatrix} = \begin{bmatrix} J_{d11} - R_{d11} & -J_{d21}^T - R_{d21}^T \\ J_{d21} - R_{d21} & J_{d22} - R_{d22} \end{bmatrix} \begin{bmatrix} \partial_1 H_d \\ \partial_2 H_d \end{bmatrix},$$

where each $J_{d..}$ and $R_{d..}$ represents the interconnection and dissipative terms of the J_d and R_d matrices, respectively. This implies that J_{d11} and J_{d22} must be skew-symmetric and similarly $R_{d11} = R_{d11}^T \geq 0$ and $R_{d22} = R_{d22}^T \geq 0$. Hence, the desired interconnection and damping matrices are

$$J_d = \begin{bmatrix} J_{d11} & -J_{d21}^T \\ J_{d21} & J_{d22} \end{bmatrix}, \quad R_d = \begin{bmatrix} R_{d11} & R_{d21}^T \\ R_{d21} & R_{d22} \end{bmatrix}.$$

Equaling the first x_1 rows of both systems yields the IDA-PBC matching equation

$$f_1 = (J_{d11} - R_{d11})\partial_1 H_d + (-J_{d21}^T - R_{d21}^T)\partial_2 H_d. \tag{3.23}$$

Assume that this equation can be solved, giving J_d, R_d and H_d satisfying the proper structural and control objective conditions. Substituting then into the equation coming from the last x_2 rows, one gets the feedback control

$$u = g^{-1}\left[(J_{d21} - R_{d21})\partial_1 H_d + (J_{d22} - R_{d22})\partial_2 H_d - f_2\right].$$

Assume now that the system (3.22) depends on some uncertain constant parameters ξ, for which we assume nominal values $\hat{\xi}$. The unknown parameters creep into the formalism

through f_i (and f_u), making the solution to the matching equation (3.23) depend on them, and also through the desired values x_1^*, which appear in H_d and which may depend on ξ due to the fact that they must obey $f_1(x_1^*, x_2^*) = 0$. Hence, the nominal control is given by

$$\hat{u} = \hat{g}^{-1}\left[(\hat{J}_{d21} - \hat{R}_{d21})\partial_1\hat{H}_d + (\hat{J}_{d22} - \hat{R}_{d22}\partial_2\hat{H}_d - \hat{f}_2\right].$$

The closed-loop system computed with the nominal control is

$$\begin{aligned} \dot{x}_1 &= (J_{d11} - R_{d11})\partial_1 H_d + (-J_{d21}^T - R_{d21}^T)\partial_2 H_d, \\ \dot{x}_2 &= f_2 - g\hat{g}^{-1}\hat{f}_2 + g\hat{g}^{-1}\left[(\hat{J}_{d21} - \hat{R}_{d21})\partial_1\hat{H}_d + (\hat{J}_{d22} - \hat{R}_{d22})\partial_2\hat{H}_d\right]. \end{aligned} \tag{3.24}$$

In the equation for x_1, (3.24), we can change H_d by $\hat{H}_d$ and put the balance terms into δ_1; denoting $\delta_2 = f_2 - g\hat{g}^{-1}\hat{f}_2$, we get a system of the form

$$\begin{bmatrix} \dot{x}_1 \\ \dot{x}_2 \end{bmatrix} = \begin{bmatrix} B_{11} & B_{12} \\ B_{21} & B_{22} \end{bmatrix} \begin{bmatrix} \partial_1\hat{H}_d \\ \partial_2\hat{H}_d \end{bmatrix} + \begin{bmatrix} \delta_1 \\ \delta_2 \end{bmatrix}.$$

The components of δ_1 can be made proportional to components of $\partial_2\hat{H}_d$ by dividing by the corresponding factors; likewise, the components of δ_2 can be made proportional to components of $\partial_1\hat{H}_d$ (one has a large amount of freedom in selecting the components of $\partial\hat{H}_d$ to which the extra terms are made proportional). After doing this, one gets

$$\begin{bmatrix} \dot{x}_1 \\ \dot{x}_2 \end{bmatrix} = \begin{bmatrix} B_{11} & B_{12} + \tilde{B}_{12} \\ B_{21} + \tilde{B}_{21} & B_{22} \end{bmatrix} \begin{bmatrix} \partial_1\hat{H}_d \\ \partial_2\hat{H}_d \end{bmatrix} \equiv \hat{A}_d\partial\hat{H}_d. \tag{3.25}$$

Notice that there are no singularities in the differential equations (3.25), since the singular terms in $\hat{A}_d$ are canceled by $\partial\hat{H}_d$.

Since any matrix can be decomposed into symmetric and skew-symmetric parts, we write

$$\hat{A}_d = \hat{J}_d - \hat{R}_d, \quad \hat{J}_d^T = -\hat{J}_d, \quad \hat{R}_d^T = \hat{R}_d.$$

Due to the $\tilde{B}_{21}$ and $\tilde{B}_{12}$ terms, the corresponding elements of $\hat{J}_d$ and $\hat{R}_d$ will contain terms which are singular at $x_1 = \hat{x}_1^*$ or $x_2 = x_2^*$. This is no formal problem for $\hat{J}_d$, but the presence of off-diagonal singular terms in $\hat{R}_d$ will destroy its positive semidefiniteness at least in a neighborhood of $(\hat{x}_1^*, x_2^*)$. Notice, however, that due to the presence of δ_1, δ_2 the closed-loop system has fixed points which differ from $(\hat{x}_1^*, x_2^*)$; if $\hat{R}_d$ is positive semidefinite in a neighborhood of the closed loop fixed points, LaSalle's theorem can still be invoked to proof local asymptotic stability, albeit not for the desired regulation point.

In order to ensure the regularization objective in presence of the unknown parameter, an integral term is introduced in basic control theory. For relative degree one outputs, this can be given a Hamiltonian form as well (see previous subsection). Keeping the unknown parameters assumption, we can rewrite the closed-loop system as follows. First of all, we write $u = \hat{u} + v$ in the original system. This yields

$$\dot{x} = (\hat{J}_d - \hat{R}_d)\partial_x\hat{H}_d + gv.$$

Because of $\partial_2 H_d|_{x_2=x_2^*} = 0$, we can enlarge the state space with $z \in \mathbb{R}^u$ so that

$$\dot{z} = -a\partial_2 H_d = -a\partial_2\hat{H}_d,$$

with $a = a^T \in \mathbb{R}^{m\times m}$ also diagonal and positive definite. The closed-loop enlarged system can be written as

$$\begin{bmatrix} \dot{x}_1 \\ \dot{x}_2 \\ \dot{z} \end{bmatrix} = \begin{bmatrix} \hat{J}_d - \hat{R}_d & 0 \\ 0 \quad -a^T & a \\ & 0 \end{bmatrix} \partial \hat{H}_{dz},$$

where

$$\hat{H}_{dz} = \hat{H}_d + \frac{1}{2} z^T z.$$

As discussed in subsection 3.4.1, due to the equation for $\dot{z}$, the only fixed points of the new closed-loop system are those with $x_2 = x_2^*$. The equation for $\dot{x}_1$ determines then x_1^* in terms of x_2^* and the actual parameter values; finally, the equation for $\dot{x}_2$ sets the equilibrium value of z, z^*, in terms of the nominal parameter values. However,

$$\hat{R}_{dz} = \begin{bmatrix} \hat{R}_d & 0 \\ & 0 \\ 0 \quad 0 & 0 \end{bmatrix}$$

has the same singularity problems that $\hat{R}_d$ in a neighborhood of x_u^*, and a proof of stability based on LaSalle's theorem cannot be given. Nevertheless, we will present an example in the next Section where the desired regulation point seems to be asymptotically stable.

Example 3.16: the toy model again

To illustrate the quite general previous remarks, consider the toy model studied in subsection 3.3.1, equation (3.11),

$$\begin{aligned} \dot{x}_1 &= -x_1 + \xi x_2^2, \\ \dot{x}_2 &= -x_1 x_2 + u, \end{aligned}$$

where $\xi > 0$ is an uncertain parameter. The control objective is to regulate x_2 to a desired value x_2^d. The IDA-PBC control law obtained was (3.13),

$$u = x_1 x_2 - \gamma \xi (x_1 - x_1^*)(x_2 + x_2^d) - \frac{r}{\gamma}(x_2 - x_2^d).$$

This control law yields a closed-loop system which is Hamiltonian with (J_d, R_d, H_d), and which has (x_1^*, x_2^d) as a globally asymptotically stable equilibrium point. However, if we use an estimated value $\hat{\xi}$ of the uncertain parameter ξ, the feedback control is

$$\hat{u} = x_1 x_2 - \gamma \hat{\xi} (x_1 - \hat{x}_1^*)(x_2 + x_2^d) - \frac{r}{\gamma}(x_2 - x_2^d),$$

where

$$\hat{x}_1^* = \hat{\xi}(x_2^d)^2 = \frac{\hat{\xi}}{\xi} x_1^*.$$

For later convenience, we also define

$$\hat{\alpha} = \gamma \hat{\xi}(x_2 + x_2^d).$$

Using this $\hat{u}$, the closed-loop system equation for $\dot{x}_2$ is

$$\begin{aligned}\dot{x}_2 &= -\gamma\hat{\xi}(x_1-\hat{x}_1^*)(x_2+x_2)-\frac{r}{\gamma}(x_2-x_2)\\ &= -\hat{\alpha}(x_1-\hat{x}_1^*)-r\frac{1}{\gamma}(x_2-x_2^d)\\ &= -\hat{\alpha}\partial_1\hat{H}_d-r\partial_2\hat{H}_d,\end{aligned}$$

where

$$\hat{H}_d=\frac{1}{2}(x_1-\hat{x}_1^*)^2+\frac{1}{2\gamma}(x_2-x_2^d)^2.$$

The equation for $\dot{x}_1$ is not changed by the feedback, but can be rewritten as

$$\begin{aligned}\dot{x}_1 &= -x_1+\xi x_2^2\\ &= -(x_1-\hat{x}_1^*)-\hat{x}_1^*+\hat{\xi}x_2^2+(\xi-\hat{\xi})x_2^2\\ &= -\partial_1\hat{H}_d+\hat{\xi}(x_2+x_2^d)(x_2-x_2^d)+(\xi-\hat{\xi})x_2^2\\ &= -\partial_1\hat{H}_d+\hat{\alpha}\frac{1}{\gamma}(x_2-x_2^d)+(\xi-\hat{\xi})x_2^2\\ &= -\partial_1\hat{H}_d+\hat{\alpha}\partial_2\hat{H}_d+(\xi-\hat{\xi})x_2^2.\end{aligned}$$

These two equations can be cast into Hamiltonian form as

$$\begin{aligned}\begin{bmatrix}\dot{x}_1\\ \dot{x}_2\end{bmatrix} &= \begin{bmatrix}-1 & \hat{\alpha}+\gamma(\xi-\hat{\xi})\frac{x_2^2}{x_2-x_2^d}\\ -\hat{\alpha} & -r\end{bmatrix}\begin{bmatrix}\partial_1\hat{H}_d\\ \partial_2\hat{H}_d\end{bmatrix}\\ &= \hat{A}_d\partial\hat{H}_d=(\hat{J}_d-\hat{R}_d)\partial\hat{H}_d,\end{aligned}$$

where $\hat{J}_d$ is the skew-symmetric part, giving the closed-loop interconnection matrix, and

$$\hat{R}_d=-\frac{1}{2}(\hat{A}_d+\hat{A}_d^T)=\begin{bmatrix}1 & -\frac{\gamma}{2}\frac{(\xi-\hat{\xi})x_2^2}{x_2-x_2^d}\\ -\frac{\gamma}{2}\frac{(\xi-\hat{\xi})x_2^2}{x_2-x_2^d} & r\end{bmatrix}.$$

One has

$$\begin{aligned}\text{tr }\hat{R}_d &= 1+r>0,\\ \det\hat{R}_d &= r-\frac{\gamma^2}{4}\frac{(\xi-\hat{\xi})^2}{(x_2-x_2^d)^2}x_2^4.\end{aligned}$$

Hence, in order to ensure that $\hat{R}_d\geq 0$, it is necessary that

$$\frac{(x_2-x_2^d)^2}{x_2^4}\geq\frac{\gamma^2(\xi-\hat{\xi})^2}{4r},\tag{3.26}$$

which is globally true if $\hat{\xi}=\xi$ but fails in a neighborhood of $x_2=x_2^d$, as well as for $|x_2|$ large enough, if $\xi\neq\hat{\xi}$.

Notice that, for $\hat{\xi}\neq\xi$, the closed-loop system does not have $x_2=x_2$, $x_1=\hat{x}_1^*$ as a fixed point, even though these are critical points of $\hat{H}_d$, due to the $1/(x_2-x_2^d)$ term in $\hat{A}_d$. In

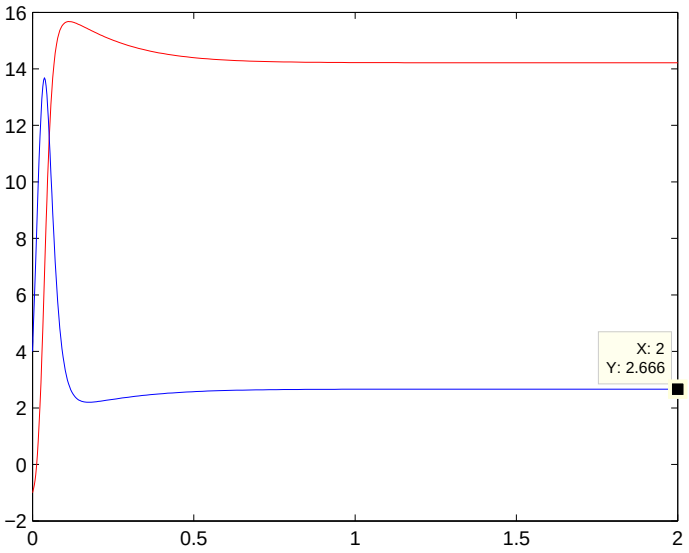

Figure 3.15: Simulation results: IDA-PBC controller for a toy model.

general, due to the state dependence of $\hat{A}_d$, other solutions may appear anyway. In fact, computing the fixed points yields the relation (depending only on the actual value of ξ)

$$x_1 = \xi x_2^2,$$

while the value of x_2 comes from the solutions to

$$0 = \gamma^2 \hat{\xi}(\xi x_2^2 - \hat{x}_1^*)(x_2 + x_2^d) + r(x_2 - x_2^d).$$

If $\hat{\xi} = \xi$, one gets

$$\gamma^2 \xi^2 (x_2^2 - (x_2^d)^2)(x_2 + x_2^d) + r(x_2 - x_2^d) = 0$$

which only has a real solution, namely $x_2 = x_2^d$. For $\xi \neq \hat{\xi}$ one has, in general, three solutions, at least one of them real, all different from x_2^d.

Figure 3.15 shows a simulation of the controller. The asymptotic value of x_2 is ~ 2.666 instead of $x_2^d = 2$, while x_1 goes to $\xi \times (2.666)^2$, as expected. As discussed in this Chapter, local asymptotic stability can be proved using LaSalle's theorem, but extensive simulations with very broad initial conditions seem to indicate that the stability is in fact global.

Following the general theory, an integral term is introduced next, so that the equation for x_2 gets modified by an az term while the dynamics of z is

$$\dot{z} = -a\frac{1}{\gamma}(x_2 - x_2^d).$$

All the fixed points of the closed-loop system have $x_2 = x_2^d$; from the equation for $\dot{x}_1$, one gets again $x_1 = x_1^* = \xi(x_2^d)^2$. Finally, the equation for $\dot{x}_2$ determines now the fixed

point value of z, z^*, which depends on the nominal value $\hat{\xi}$, instead of determining the fixed point for x_2.

Figure 3.16 shows a simulation of the new controller, for the same parameter values than the simulation for the old controller and $a = 50$. The variable z, the integral of the error in x_2, starts from zero an goes asymptotically to z^*. A longer transitory appears, as is characteristic of integral controllers. Simulations with initial values in a wide range of points, seem to point to the global stability of the closed loop system.

However, if r is decreased oscillations do appear. For instance, for $r = 20$ and the same values of all the other parameters, one gets the response displayed in Figure 3.17. The disappearance of the oscillations when r is increased corresponds to a (reversed) Hopf bifurcation. In fact, linearizing the closed loop system around $(\xi(x_2^d)^2, x_2^d, z^*)$ yields a system which is asymptotically stable as long as

$$\frac{r}{\gamma} + \gamma\hat{\xi}(x_2^d)^2(\xi - \hat{\xi}) - (\xi - \gamma\hat{\xi})^2(x_2^d)^2 > 0,$$

which is true for r sufficiently large. Numerical simulations seem to imply that the fixed point of the nonlinear system is globally asymptotically stable. Computing the time derivative of $\hat{H}_{dz}$,

$$\frac{\mathrm{d}}{\mathrm{d}t}\hat{H}_{dz} = -(x_1 - \hat{x}_1^*)^2 + (\xi - \hat{\xi})x_2^2(x_1 - \hat{x}_1^*) - \frac{r}{\gamma^2}(x_2 - x_2^d)^2, \tag{3.27}$$

it can be seen that the region where (3.27) is nonpositive is much larger than what is implied by (3.26), due to the state-space dependence of the closed-loop dissipation matrix; in fact, for r large enough, the nonpositive region is pushed away from the desired regulation point, except for a bounded shrinking region whose boundary contains the later and which contains most of the periodic orbit. Although the details are quite particular to this example, we hope to obtain some insight into any existing mechanism which could be generalized.

3.4.3 Robust control via structure modification

As discussed in the previous Section, it is not clear how to generalize the integral extension for higher relative degree outputs in the PCHS framework. We present here a different approach, which can be applied to a larger class of systems. Examples include the DC motor, the electrical part of a doubly-fed induction machine or the buck power converter.

Consider a dynamical system of the form

$$\begin{cases} \dot{x}_o = f_o(x_o, x_u, \xi) \\ \dot{x}_u = f_u(x_o, x_u) + g(x_o, x_u)u \end{cases} \tag{3.28}$$

where $x_o \in \mathbb{R}^o$ are higher order relative degree outputs, $x_u \in \mathbb{R}^u$, $u \in \mathbb{R}^p$ are the controls and ξ is an uncertain parameter. To simplify the presentation we consider $p = u = o$ and that g is full rank.

As a control target we fix a desired x_o^d, which implies that the fixed point value of x_u is given by the following equation

$$f_o(x_o^d, x_u^*, \xi) = 0, \tag{3.29}$$

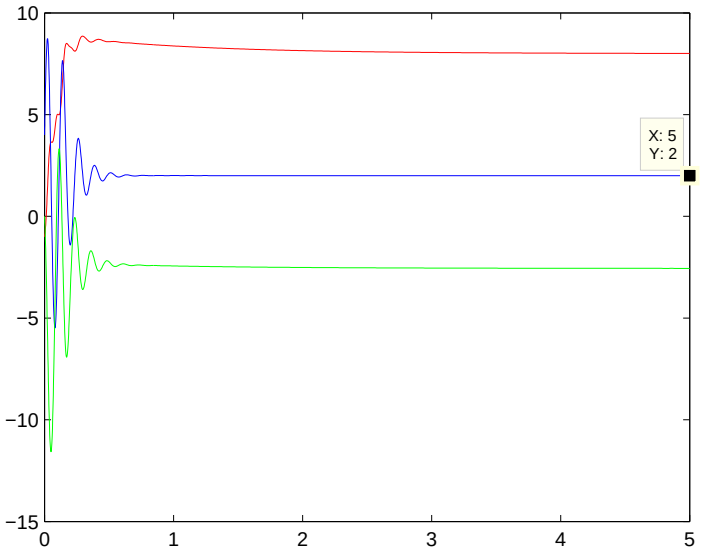

Figure 3.16: Simulation results: IDA-PBC+integral controller (with $r = 50$) for a toy model.

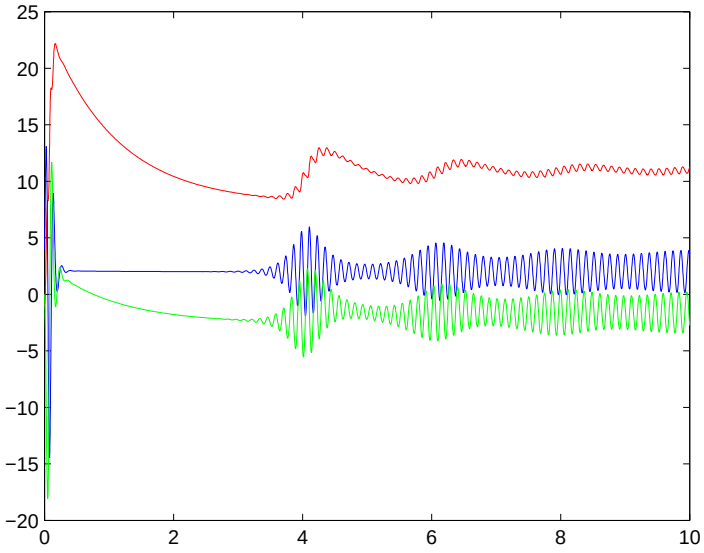

Figure 3.17: Simulation results: IDA-PBC+integral controller (with $r = 20$) for a toy model.

and depends thus on the uncertain parameter ξ.

Applying the IDA-PBC technique, we match the system to the desired port Hamiltonian structure, where $(J_d - R_d)$ is partitioned as

$$\begin{bmatrix} \dot{x}_o \\ \dot{x}_u \end{bmatrix} = \begin{bmatrix} J_{doo} - R_{doo} & -J_{duo}^T - R_{duo}^T \\ J_{duo} - R_{duo} & J_{duu} - R_{duu} \end{bmatrix} \begin{bmatrix} \partial_o H_d \\ \partial_u H_d \end{bmatrix}.$$

Each $J_{d..}$ and $R_{d..}$ represents the interconnection and dissipative terms of the J_d and R_d matrices, respectively. This implies that J_{doo} and J_{duu} must be skew-symmetric and similarly $R_{doo} = R_{doo}^T \geq 0$ and $R_{duu} = R_{duu}^T \geq 0$. Hence, the desired interconnection and damping matrices are

$$J_d = \begin{bmatrix} J_{doo} & -J_{duo}^T \\ J_{duo} & J_{duu} \end{bmatrix}, \quad R_d = \begin{bmatrix} R_{doo} & R_{duo}^T \\ R_{duo} & R_{duu} \end{bmatrix}.$$

Notice that we need a H_d such that $\partial H_d|_{x=x^*} = 0$ to obtain an equilibrium point in $x^* = (x_o^d, x_u^*)$. Equaling the u rows of the IDA-PBC matching equation (4.42) the control law yields

$$u = g^{-1} \left[(J_{duo} - R_{duo})\partial_o H_d + (J_{duu} - R_{duu})\partial_u H_d - f_u \right].$$

Since H_d is a free function, it is chosen so that $\partial_o H_d$ does not depend on ξ (Notice that x_u^* depends on it, equation (3.29)). In the same way, ξ can appear in $\partial_u H_d$ through x_u^*, which can be removed from the control law setting

$$J_{duu} - R_{duu} = 0,$$

and the robustified IDA-PBC control law is

$$u = g^{-1} \left[(J_{duo} - R_{duo})\partial_o H_d - f_u \right].$$

As we set $R_{duu} = 0$, again Schur's complement shows that in order to keep the semi-positiveness of R_d, we are forced to $R_{duo} = 0$, and consequently

$$u = g^{-1} \left[J_{duo}\partial_o H_d - f_u \right]. \tag{3.30}$$

From the o rows of the IDA-PBC matching equation (4.42), the following equation must be satisfied, were we fixed $R_{duo} = 0$,

$$f_o = (J_{doo} - R_{doo})\partial_o H_d - J_{duo}^T \partial_u H_d. \tag{3.31}$$

Selecting J_{duo} full rank,

$$\partial_u H_d = -(J_{duo}^T)^{-1} \left[f_o - (J_{doo} - R_{doo})\partial_o H_d \right]. \tag{3.32}$$

Rewriting f_o as

$$f_o = A(x)\partial_o H_d + B(x_u),$$

and choosing $(J_{doo} - R_{doo})$ so that

$$A(x) = J_{doo} - R_{doo},$$

the PDE (3.32) simplifies to

$$\partial_u H_d = -(J_{duo}^T)^{-1} B(x_u).$$

Notice that J_{duo} must be a function of x_u only, $J_{duo} = J_{duo}(x_u)$. Fixing a part of the Hamiltonian and then finding the rest of H_d solving the PDE was also proposed in [61]. Stability can be discussed, using LaSalle's theorem. Dissipativity is assured if

$$R_{doo} = R_{doo}^T > 0.$$

This is equivalent to

$$A(x) + A(x)^T < 0.$$

Notice that this condition depends only on f_o, irrespectively of u. Convergence to the equilibrium point, defined by $\partial_u H_d|_{x=x^*} = 0$, follows from the condition

$$\partial^2 H_d\big|_{x=x^*} > 0,$$

or, in other words,

$$\partial_u \left(-(J_{duo}^T)^{-1} B(x_u)\right)\big|_{x=x^*} > 0.$$

We can summarize this Section in the following Proposition.

Proposition 3.17. *Consider a dynamical system given by (3.28), so that f_o can be expressed as,*

$$f_o = A(x)\partial_o H_d + B(x_u) \tag{3.33}$$

where $\partial_o H_d$ is a design function of x_o such that

$$\partial_o H_d(x_o)|_{x_o=x_o^d} = 0$$

and

$$\partial_o^2 H_d(x_o)\big|_{x_o=x_o^d} > 0. \tag{3.34}$$

Then the control law

$$u = g^{-1}\left[J_{duo}(x_u)\partial_o H_d - f_u\right], \tag{3.35}$$

where $J_{duo}(x_u)$ is another design function of x_u, is robustly stable in front of variations of ξ as long as

$$A(x) + A^T(x) < 0, \tag{3.36}$$

$$\left(-(J_{duo}^T)^{-1} B(x_u)\right)\big|_{x=x^*} = 0, \tag{3.37}$$

and

$$\partial_u \left(-(J_{duo}^T)^{-1} B(x_u)\right)\big|_{x=x^*} > 0. \tag{3.38}$$

Notice that condition (3.36) implies that the dynamics of the output variables x_o is dissipative, and this is the only dissipation of the closed-loop system (due to $R_{duu} = R_{duo} = 0$).

Example 3.18: the toy model

Consider once more the toy model studied in subsection 3.3.1, equation (3.11), where $\xi > 0$ is an uncertain parameter. In this case, differing from the previous subsection, the desired output is fixed by x_1^d. Notice that x_1 is now a relative degree two output, and the integral term discussion is not clear.

Applying the classical IDA-PBC method to the system, the following feedback control law is obtained[2]

$$u = x_1 x_2 - \gamma\xi(x_1 - x_1^d)(x_2 + x_2^*) - \frac{r}{\gamma}(x_2 - x_2^*),$$

where $r > 0$, $\gamma > 0$ are control parameters. Notice that the control law u depends on x_1^d and x_2^*, where x_2^* is function of ξ,

$$x_2^* = \sqrt{\frac{1}{\xi}x_1^d}.$$

In this case the control law is not robust with respect to an uncertain $\hat{\xi}$.

Let us calculate a new controller following the previous discussion. In this case the x_o output variable is x_1 and the x_u variable is x_2. First we fix $\partial_o H_d$ as

$$\partial_o H_d = x_1 - x_1^d$$

which ensures conditions (3.34) and (3.35). Then from (3.33), $A(x)$ and $B(x_u)$ must be

$$A(x) = -1 \quad B(x_u) = \xi(x_2^2 - x_2^{*2}).$$

Notice that condition (3.36) is achieved.

The easiest choice of J_{duo} is a free constant, for instance $k > 0$, but for this nonlinear example it is necessary to add a more complicated $a(x_2)$ function[3]. Then the final choice is

$$J_{duo} = J_{duo}^T = -a(x_2)k$$

with $k > 0$ and

$$a(x) = \begin{cases} 1, & x_2 > 0 \\ b, & x_2 = 0 \\ -1, & x_2 < 0 \end{cases} \tag{3.39}$$

where $b \in [-1, 1]$ is a parameter that would be used to choose the equilibrium point of x_2 (see discussion on the closed-loop dynamics at the end of the example). This selection ensures conditions (3.37)

$$\frac{1}{a(x_2)k}\xi(x_2^2 - x_2^{*2})\Big|_{x_2 = x_2^*} = 0$$

and (3.38),

$$\left(\frac{1}{a(x_2)k}\xi(x_2^2 - x_2^{*2})\right)\Big|_{x_2 = x_2^*} > 0$$

Finally the controller is obtained from (3.30) yields

$$u = x_1 x_2 - ak(x_1 - x_1^d). \tag{3.40}$$

[2]This control law is the same than (3.13), with the desired output variable x_1^d instead x_2^d.

[3]The $a(x)$ function is included to avoid stability restrictions on the space-state. The same procedure with $a = 1$ implies

$$\partial^2 H_d|_{x=x^*} = \begin{bmatrix} 1 & 0 \\ 0 & 2\frac{\xi}{k}x_2^* \end{bmatrix}$$

which is negative for $x_2^* < 0$. Consequently, the globally asymptotically stability is not achieved.

The example seen as a classic IDA-PBC design

This design can be also obtained following the traditional IDA-PBC method in order to show the Hamiltonian structure of the closed–loop system. Consider the matching equation of the system (3.11) with the PCHS dynamics (3.4) where

$$J_d = \begin{bmatrix} 0 & a(x_2)k \\ -a(x_2)k & 0 \end{bmatrix}, \quad R_d = \begin{bmatrix} r_c & 0 \\ 0 & 0 \end{bmatrix}$$

where $k > 0$, $a(x_2)$ is described in (3.39) and a Hamiltonian function such that

$$\partial_x H_d = \begin{bmatrix} x_1 - x_1^d \\ \partial_{x_2} H_d \end{bmatrix}. \tag{3.41}$$

From the second row of the matching equation we obtain the same robust control law as (3.40)

$$u = x_1 x_2 - ak(x_1 - x_1^d)$$

which does not depend on ξ. From the first row we must compute $\partial_{x_2} H_d$ and verify the stability properties of the closed loop system. The matching equation yields

$$-x_1 + \xi x_2^2 = -r_c(x_1 - x_1^d) + ak\partial_{x_2} H_d$$

and, using $r_c = 1$ and $x_1^d = \xi x_2^{*2}$,

$$\partial_{x_2} H_d = \frac{\xi}{ak}(x_2^2 - x_2^{*2}). \tag{3.42}$$

To show stability, with the desired structure (3.4) and $J_d = -J_d^T$, $R_d = R_d^T > 0$ we only need positiveness of the Hessian of H_d evaluated at x^*,

$$\partial_x^2 H_d|_{x=x^*} = \begin{bmatrix} 1 & 0 \\ 0 & 2\frac{\xi}{k} a(x_2^*) x_2^* \end{bmatrix},$$

which is true for all x_2^*, as long as $k > 0$ and $\xi > 0$. Notice that

$$\partial_{x_2}^2 H_d = \frac{\xi}{k}\left(\Theta(x_2)(x_2^2 - x_2^{*2}) + 2a(x_2)x_2\right),$$

where $\Theta(x_2)$ is the Heaviside function.

The Hamiltonian function can be found integrating $\partial_x H_d$ (equation (3.41) with (3.42))

$$H_d = a(x_2)\frac{\xi}{k} x_2 \left(\frac{1}{3}x_2^2 - x_2^{*2}\right) + \frac{1}{2}(x_1 - x_1^d)^2,$$

which has two local minima, both with first coordinate x_1^d. H_d is depicted in Figure 3.18 (using the same simulation parameters than for Figures 3.19 and 3.20). Notice that two equilibrium points appear, given by

$$x_2^* = \pm\sqrt{\frac{1}{\xi} x_1^d},$$

and these points yield the same value for x_1^d. In the *classical* controller this ambiguity did not appear, basically because we were fixing the *desired* value of x_2^*, while in the robust controller both values of x_2 are possible.

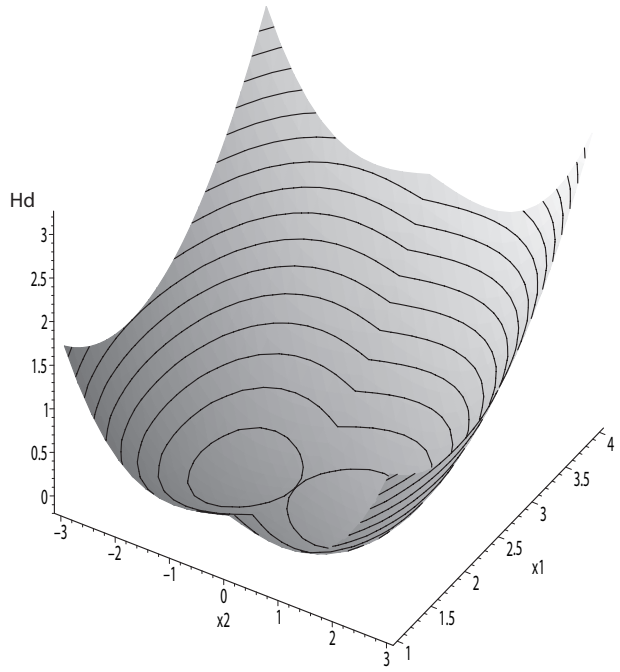

Figure 3.18: Desired Hamiltonian function, H_d.

Simulations

Figures 3.19 and 3.20 show simulation results testing both controllers, the robust method presented above and the classic IDA-PBC. The parameters are $\xi = 2$, $\hat{\xi} = 1$, with initial conditions $x(0) = (0, -1.5)$, and the desired output is $x_1^d = 2$. The control parameter for the robust control law is $k = 10$, while for the classical IDA-PBC $r = 1$ and $\gamma = 1$ are selected.

The robust controller achieves the desired value of x_1 even with a wrong parameter estimation, while the classical IDA-PBC controller is sensible to the ξ variations. Notice that the variations on $\hat{\xi}$ change the x_2^* equilibrium point.

Study of the closed-loop dynamics

Now we focus on to study of the dynamical behavior of the controller designed above. Fig. 3.21 shows the phase portrait of the closed–loop system (the values of the parameters are as above).

Two stable fixed points,$x^* = (2, \pm 1)$, are present. To select x_2^*, let us to write the system (3.11) with the feedback control law (3.40),

$$\begin{cases} \dot{x}_1 = -x_1 + \xi x_2^2 \\ \dot{x}_2 = -ak(x_1 - x_1^d) \end{cases}$$

The dynamics after reaching $x_2 = 0$ there is described by

$$\dot{x}_1 = -x_1,$$

so x_1 tends to $x_1 = 0$, and simultaneously the x_2 dynamics is

$$\dot{x}_2 = -ak(x_1 - x_1^d)$$

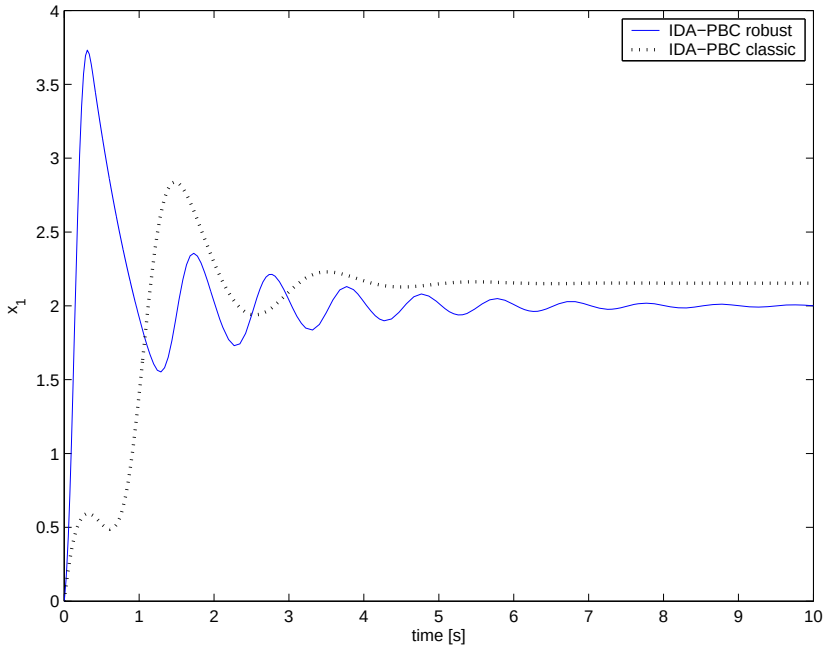

Figure 3.19: Comparison between the *robust method* and the *classic* IDA-PBC, behaviour of x_1.

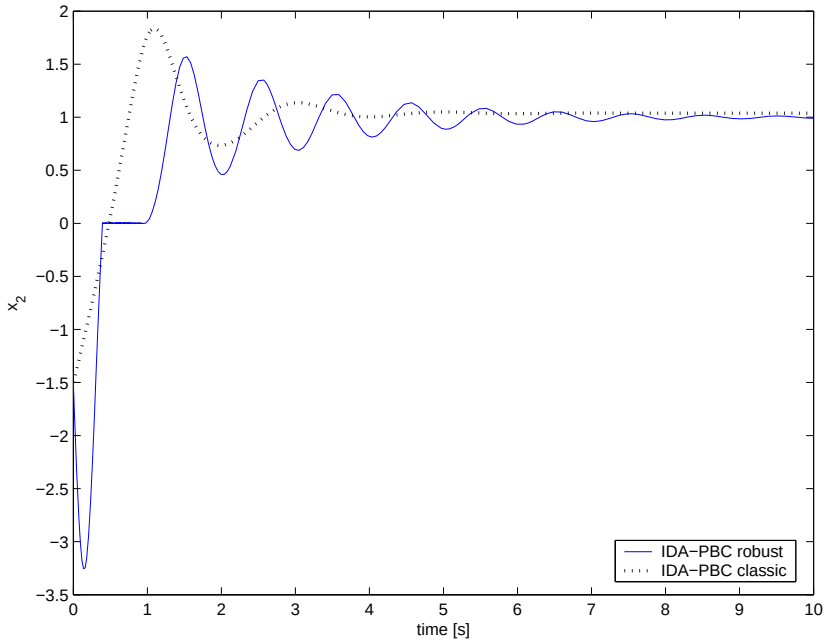

Figure 3.20: Comparison between the *robust method* and the *classic* IDA-PBC, behaviour of x_2.

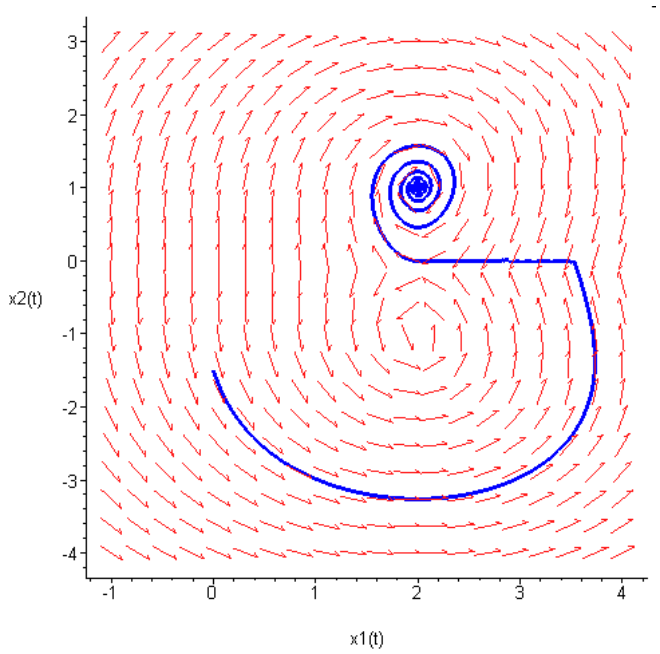

Figure 3.21: State space; trajectory and vector field.

where $k > 0$ and $a(x_2) = b$ with $b \in [-1, 1]$. Notice that for $x_1 > x_1^d$, and sufficiently far of the equilibrium point, $x_2 = 0$ is an attractor set. Besides, for $x_1 < x_1^d$ and $x_2 = 0$ the dynamics of x_2 for $b = 1$ is increasing, while if $b = -1$ the dynamics of x_2 decreases. In other words, for $b = 1$

$$\lim_{t\to\infty} x_2 = +\sqrt{\frac{1}{\xi}x_1^d}$$

and for $b = -1$

$$\lim_{t\to\infty} x_2 = -\sqrt{\frac{1}{\xi}x_1^d}.$$

Figure 3.22 shows a phase portrait of two different simulations, for $b = 1$ with a continuous line and $b = -1$ with a dotted line. The behaviour is as expected from the discussion above, for $b = 1$, x_2 tends to $+\sqrt{\frac{1}{\xi}x_1^d}$ while for $b = -1$ x_2 tends to $-\sqrt{\frac{1}{\xi}x_1^d}$. In Figure 3.23 the same simulations are depicted in function of time.

For numerical simulations, we modify $a(x)$ (3.39) as

$$a(x) = \begin{cases} 1, & x_2 > \epsilon \\ b, & -\epsilon < x_2 < \epsilon \\ -1, & x_2 < \epsilon \end{cases}$$

where $\epsilon > 0$ is a constant, so that numerical errors do not bring the trajectory to the wrong fixed point.

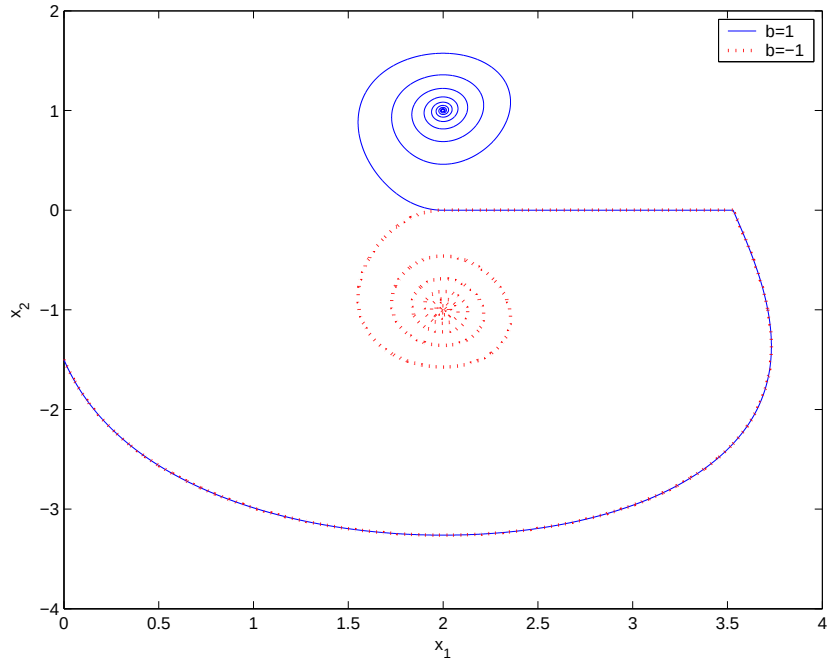

Figure 3.22: Phase portrait of x for two different b values. $b = 1$ with a continuous line and $b = -1$ with a dotted line.

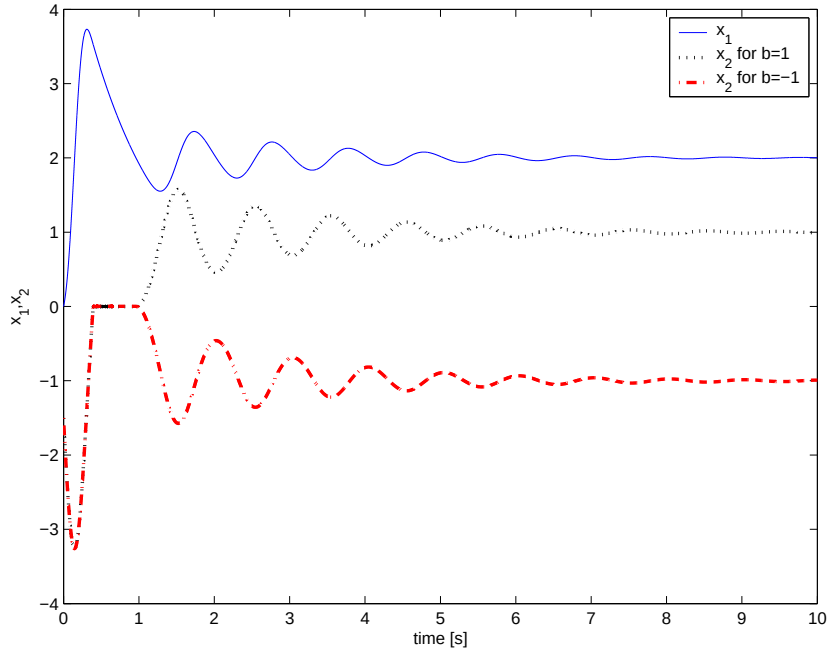

Figure 3.23: Simulations for two different b values.

Example 3.19: the DC motor

This robust IDA-PBC technique can also be applied to the DC motor speed control problem. Consider the DC motor described in Section 2.2, in PCHS form given by

$$\dot{x} = (J - R)\partial H(x) + g + g_u u$$

with $x \in \mathbb{R}^2$

$$x = [\lambda, p_m]^T,$$

and where λ is the inductor flux and p_m is the angular momentum. The interconnection, dissipation and port matrices are

$$J = \begin{bmatrix} 0 & -K \\ K & 0 \end{bmatrix} \quad R = \begin{bmatrix} r & 0 \\ 0 & B_r \end{bmatrix} \quad g = \begin{bmatrix} 0 \\ -\tau_L \end{bmatrix} \quad g_u = \begin{bmatrix} 1 \\ 0 \end{bmatrix}$$

with the control input $u = v$. r and B_r represent the electrical and mechanical losses respectively, and the Hamiltonian function is given by

$$H(x) = \frac{1}{2L}\lambda^2 + \frac{1}{2J_m}p_m^2,$$

where L is the inductance and J_m the inertia of the motor. Assume that the control objective is a desired speed ω^d and in that the unknown parameter is the external torque τ_L.

Following the procedure described in Proposition 17, where the x_o (output) variable is the mechanical speed ω and the x_u variable is the inductor current i, we choose

$$\partial_o H_d = \frac{1}{J_m}(p_m - p_m^d) = \omega - \omega^d, \tag{3.43}$$

which ensures (3.34). Now f_o from equation (3.33) can be written as

$$f_o = Ki - B_r\omega - \tau_L = A(x)(\omega - \omega^d) + B(x),$$

and into taking account $\tau_L = Ki^* - B_r\omega^d$, $A(x)$ and $B(x)$ are given by

$$A = -B_r,$$

$$B = K(i - i^*),$$

which fulfill the conditions (3.36), (3.37) and (3.38), with

$$J_{duo} = \gamma > 0. \tag{3.44}$$

Finally, the control law is obtained from (3.35),

$$u = \gamma(\omega - \omega^d) - ri - K\omega$$

with (3.43), (3.44) and

$$f_u = -ri - K\omega.$$

Figure 3.24 shows the behaviour of the DC motor with the IDA-PBC robust control law. The motor parameters are: $r = 0.05\Omega$, $L = 2mH$, $K = 0.07\text{N·m·A}^{-1}$, $B_r = 0.01\text{N·m·rad}^{-1}\text{s}^{-1}$, $J_m = 0.0006\text{Kg·m}^2$, the nominal torque is $\tau_L = 1.25\text{N·m}$ and $\gamma = 0.05$. The system starts at $\omega = 170\text{rad·s}^{-1}$ with $\omega^d = 120\text{rad·s}^{-1}$. For $t = 1\text{s}$ the desired mechanical speed is changed to $\omega^d = 170\text{rad·s}^{-1}$, and for $t = 2\text{s}$ the external torque decreases until $\tau_L = 0.25\text{N·m}$. Notice that the mechanical speed regulation is achieved even with the change of the external torque.

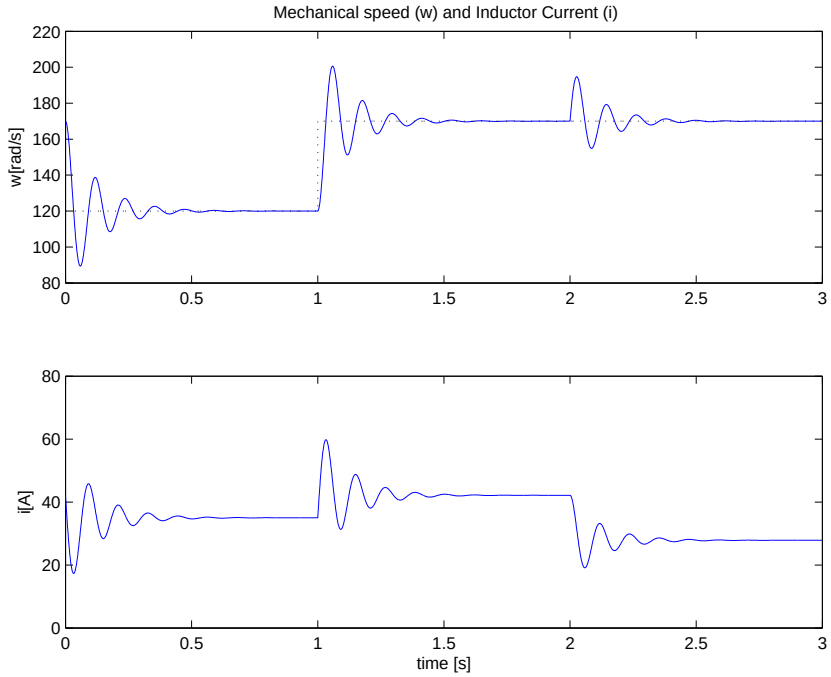

Figure 3.24: Simulations of the IDA-PBC robust for a DC motor.